Bountiful City Dichloromethane and Formaldehyde Source Apportionment Study

Jaron Hansen
Professor of Chemistry and Biochemistry
Brigham Young University
jhansen@chem.byu.edu
(801) 422-4066

Delbert J. Eatough
Professor of Chemistry and Biochemistry, Emeritus
Brigham Young University
delbert@eatough.net
(801) 375-5535

1. Background

In 2015 the Utah Division of Air Quality and Dr. Kerry Kelly conducted a year-long study to determine the concentrations and seasonal trends of formaldehyde and dichloromethane at Lindon, West Valley and Bountiful (Kuprov, 2016). Dichloromethane concentrations were found to be significantly higher at the Bountiful site than the other locations, with concentrations that would result in increased health impacts on the population (Centers for Disease Control and Prevention, 2012). To attempt to identify the probable sources of formaldehyde and dichloromethane, a 6 week-long summer, 7 week-long winter saturation study was conducted at 34 sites in the Bountiful area by Dr. Kerry Kelly and the Utah Division of Air Quality (Kelly et al., 2017 and Kelly and Daher 2017). Integrated 5-day daytime and 5-day nighttime samples were collected during the study. The data were analyzed with respect to measured concentrations and wind direction. Based on the results it was concluded that the dichloromethane emissions were intermittent. The relatively large spatial variation observed in dichloromethane concentrations led to the conclusion that the area had emission hotspots. The dichloromethane concentrations during weeks 2, 3, 4 and 6 were below the 0.3 ppb one-in-a-million cancer risk but exceeded the cancer risk during weeks 1 and 5 of the study.

More recently, Dr. Kelly has conducted a PMF analysis of historical air quality data (Jaramillo et al. 2019). Analysis of the 24-hour historical data indicates that there is a single source for dichloromethane.

In order to generate a data set with a higher time resolution compared to the above referenced past studies, a study was conducted during February through April (2019) in Bountiful.

Starting in February 2019, BYU directed an eight-week intensive campaign measuring the components expected to be important to understanding the sources of dichloromethane and formaldehyde at the Bountiful sampling site located at Bountiful Viewmont High School, 171 W. 1370 N. Bountiful, UT (EPA AIRS code: 490110004) on an hourly basis. This included the hourly average measurement of dichloromethane and other gases (focusing on PAMS compounds) measurable by the GC, which DAQ made available to BYU. $PM_{2.5}$ as measured

with an FDMS TEOM, a Sunset Carbon Monitor, an aethalometer and a BYU GC-MS Organic Aerosol Monitor (OAM) were used for the determination of fine particulate organic marker compounds. In addition, the concentrations of NO_X, NO_2 and CO were also measured by the State. It was originally intended that fine particulate composition would be measured with an AIMS (to be run by the DAQ) but that proved to not be possible due to space and power limitations in the sampling shed. In addition, the data from the Sunset instrument were not reliable and are not included in this report. This report provides a PMF analysis based on 2-hour average data. Corresponding back trajectory calculations for selected time periods based on the PMF analysis were provided by the State and their interpretation is included in this report.

The main objective of the study is the identification of sources of dichloromethane and formaldehyde. However, sources of dichloromethane will include emissions for industries using dichloromethane as a solvent, emissions from the refineries located near Bountiful and emissions from diesel traffic. To better understand this possible variety of emission sources two PMF analyses were performed, one based on the concentrations of dichloromethane and one based on $PM_{2.5}$. In both cases the EPA-PMF v5.0 software (EPA, 2014) was used for the analysis.

2. Experimental

Fine particulate mass, particulate organic markers and related gas phase species were measured all on an hourly average basis. The following two-hour averaged data were used in the PMF analysis:

2.1 Fine Particulate Mass

$PM_{2.5}$ mass was measured using an R&P Model 8599 FDMS (Filter Dynamics Measurement System) Tapered Element Oscillating Microbalance (TEOM) sampler. The FDMS TEOM measures all fine particulate mass including ammonium nitrate and semi-volatile organic material but does not measure fine particulate water. (Grover and Eatough, 2008; Grover et al., 2008)

2.2 Carbonaceous Material

Black carbon and UV absorbing carbon were determined with a seven wavelength aethalometer (Magee Scientific). The aethalometer sampled ambient air at a rate of 2.5 slpm, through 4m of anti-static tubing, with a diameter of 1/4".

2.3 Criteria Gas Phase Species

CO, O_3 and NO_x (NO, NO_2) were monitored using analyzers from the Utah Department of Air Quality (UDAQ), which included a Teledyne Advanced Pollution Instrumentation (API) gas filter correlation CO analyzer (Model 300 E), photometric ozone analyzer (Model 400 E), and T series NO_x analyzer (Model T200U) equipped with a NO_2 photolytic converter, respectively. The trace gas analyzers were calibrated bi-weekly and automated precision, zero and span (PZS) checks were performed automatically to monitor any drifts. The ambient air was drawn into a manifold at ~ 10 slpm through ~ 10 m long 1⁄2" O.D. PFA tubing to a 6-port glass manifold. The trace gas analyzers sub-sampled from this manifold at 600 – 700 sccm.

2.4 CH_2O

A Broadband Cavity Enhanced Absorption Spectrometer (BBCEAS) instrument was used to measure CH_2O and NO_2. The BBCEAS leverages long path lengths (1-5 km) by use of multi-reflections in a short instrument footprint (1-2 m). A cage system constructed of carbon-fiber tubes was employed to obtain optical alignment, with structural parts being 3-D printed (laser-sintering or extruded PLA, depending on the function of the part). Initial tests were performed with a base path of 98.5 cm and 5 cm diameter highly reflective mirrors from Advanced Thin Films (ATFilms) centered at 365 nm, with a second cavity centered at 455 nm. Light was produced by LEDEngin (blue) and Thorlabs (M340D3) LEDs centered at 450 and 340 nm, respectively, and collected at the rear of the cavity onto optical fibers. An Andor Shamrock SR-303i spectrograph with gated, intensified CCD was used as a detector in the UV region (310-400 nm range, ~0.5 nm FWHM). In the visible region, an Avantes AvaSpec-2048L was used as a detector.

Nitrogen and helium were supplied to the cavity to characterize the mirror loss as well as air and NO_2 produced from the reaction of NO with O_3 in a calibration source. The mirror reflectivity was calculated as follows:

$$R(\lambda) = 1 - d_0 \left(\frac{\frac{I_{N2}(\lambda)}{I_{He}(\lambda)} \alpha_{Ray}^{N2}(\lambda) - \alpha_{Ray}^{He}(\lambda)}{1 - I_{N2}(\lambda)/I_{He}(\lambda)} \right).$$

Where d_0 is the cavity length, I is the intensity (spectrum) in nitrogen or helium, and α is the Rayleigh scattering.

Reference spectra were acquired every two hours using an overflow value controlled by a separate Arduino circuit. Spectra were saved every minute, with signal averaging carried out in post-processing to bring noise in the fitting down. Spectra were simultaneously fitted for CH_2O and NO_2.

For ambient sampling, a 2 m long, ¼"Teflon inlet extended out of the DAQ trailer in Bountiful, UT with a 2 μm PTFE filter at the end of the inlet. Air was pulled at a total flow of 1.5 slpm at the inlet, with additional air added as purges over the mirrors. The CH_2O fitting window was narrowed to 346-357 nm due to drifts in LED/mirror matching over time at the wings of the mirror reflectivity.

2.5 Organic Marker Compound Data

The Gas Chromatography–Mass Spectrometry Organic Aerosol Monitor (GC-MS OAM) used in this study has been described previously (Cropper et al., 2018, 2019). The GC-MS OAM combines fully automated filter collection of fine particles with thermal desorption, GC and MS to quantitatively measure carbonaceous components of PM on a 90-minute averaged basis. Ambient air was pulled at 16.7 slpm through a $PM_{2.5}$ cyclone cutoff filter, with a sample collection flow rate of 8 slpm and a bypass flow of 8.7 slpm. A chemically deactivated quartz filter was utilized for collection followed by thermal desorption at 280°C into the GC-MS, and subsequent GC-MS analysis. Compounds measured by the GC-MS OAM and used in the PMF analysis included fluorene, levoglucosan (and its isomers), stearic acid, pyrene and anthracene.

2.6 GC-FID Data

A Perkin/Elmer GC-FID Clarus 580 made hourly averaged measurements of dichloromethane, benzene, toluene, ethylbenzene and xylenes (BTEX). Ambient samples were collected by use of a 2 m long, ¼"Teflon inlet extended out of the DAQ trailer in Bountiful, UT with a 2 um PTFE filter at the end of the inlet. Air flowing at 200 sccm was pulled through a preconcentrator kept at -30 °C for 45 minutes. After the collection period, the preconcentrated sample is flash heated and pushed using ultrapure He (99.999%) through an open tubular column for separation and finally detection by flame ionization detection. Built into the sampling protocol was injection of a standard gas mixture (AirGas) containing dichloromethane, benzene, toluene, ethylbenzene and xylenes once a day.

3. Data Archive

The quality inspected data used in the PMF analysis, including uncertainties, is archived at ScholarsArchive managed by Brigham Young University and can be found at https://scholarsarchive.byu.edu/cgi/preview.cgi?article=1020&context=data.

Missing data for any species are time periods when the instrument was not working.

4. Data Available for PMF Analyses

The following data were available for the PMF analysis of sources of dichloromethane.

GC measured dichloromethane and selected PAMS gases including benzene, toluene, ethylbenzene and xylene. These data are included in Figure 1.

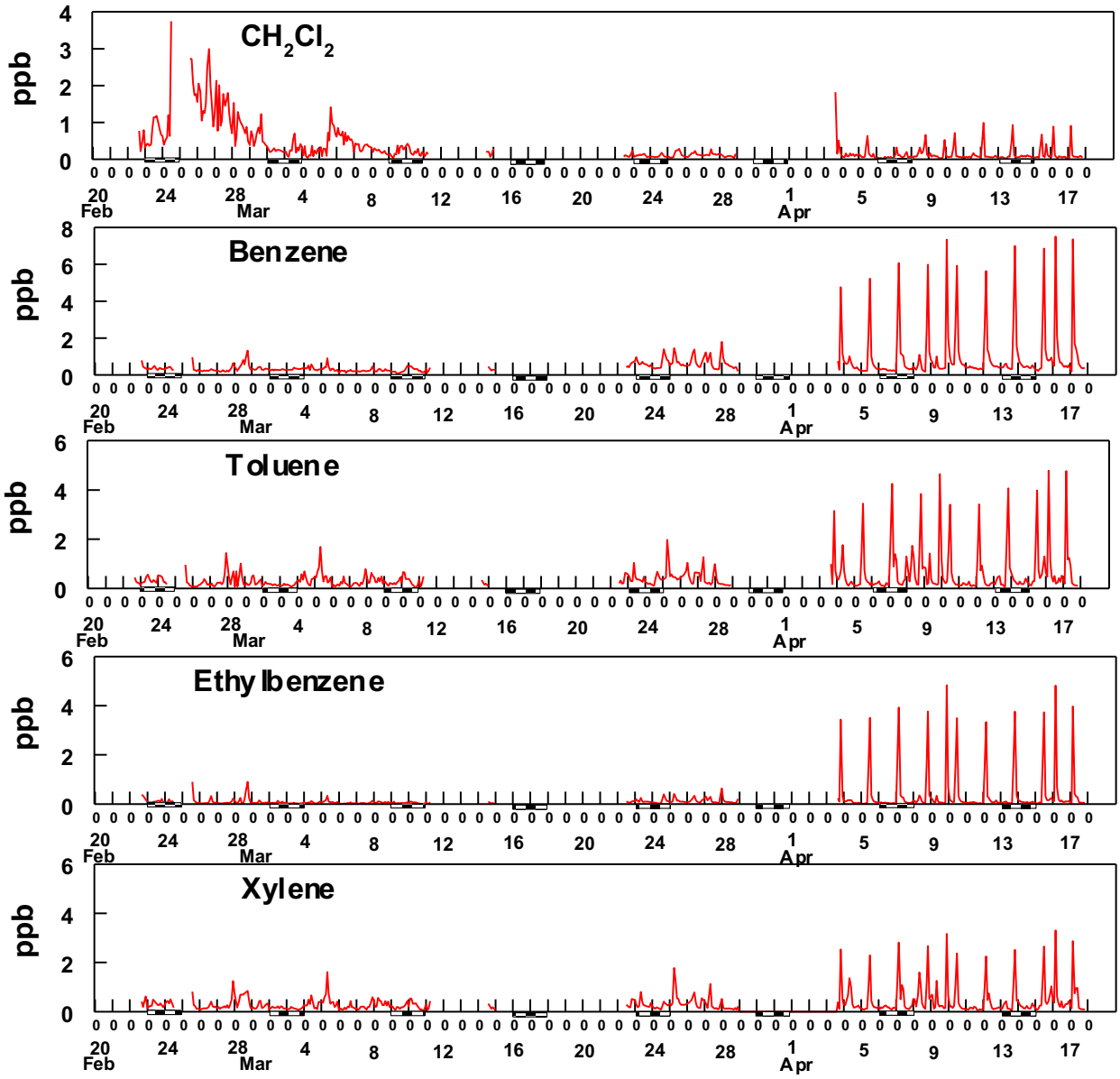

Figure 1. Two-hour average data for dichloromethane, benzene, toluene, ethylbenzene and xylene. The hash marks under the X axis indicates weekends.

The most notable feature of the data in Figure 1 is the consistency of the time patterns among the PAMS gases, suggesting they are all dominated by a single source, possibly the refineries to the west and southwest of the sampling site. Comparison of the data shown in Figure 1 with calculated back wind trajectories is given in section 9 and provides supporting evidence for the hypothesis that these species are emitted from a single source. In contrast, the diel pattern for dichloromethane is quite different with the presence of low concentrations with a pattern like that for the PAMS gases in April, but a very different pattern from these gases (and higher concentrations) in February and early March. After examination of the data the uncertainty limits for the PMF analysis for the species given in Figure 1 were selected as given in Table 1.

The uncertainly for each data point was calculated as LOD + Precision*[Species].

Table 1. Values used in the creation of the uncertainty matrix for PMF analysis of the species in Figure 1.

Value	Dichloromethane	Benzene	Toluene	Ethylbenzene	Xylene
LOD, ppb	0	0.04	0.04	0.04	0.04
Precision	4	0.10	0.10	0.10	0.10

Because it was the species being fit for the PMF analysis the uncertainty of dichloromethane was taken to be four time the measured concentration (Polissar et al., 1998).

Species related to the possible presence of dichloromethane and included in the PMF analysis of dichloromethane are given in Figures 2 and 3.

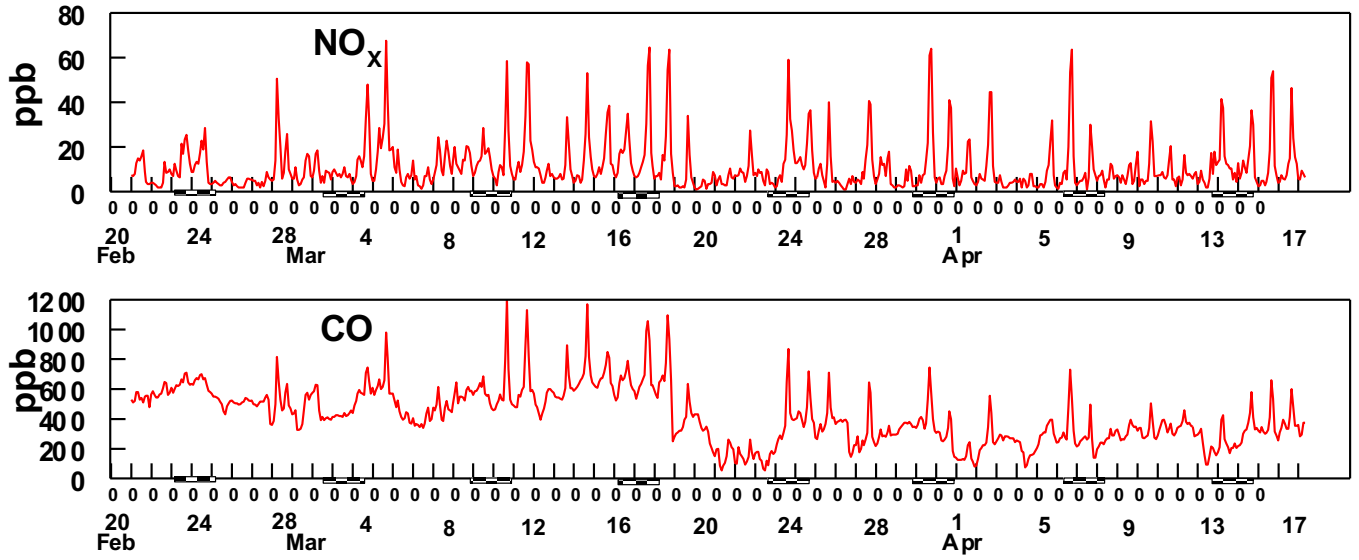

Figure 2. Two-hour average data for NO_X. and CO. The hash marks under the X axis indicate weekends.

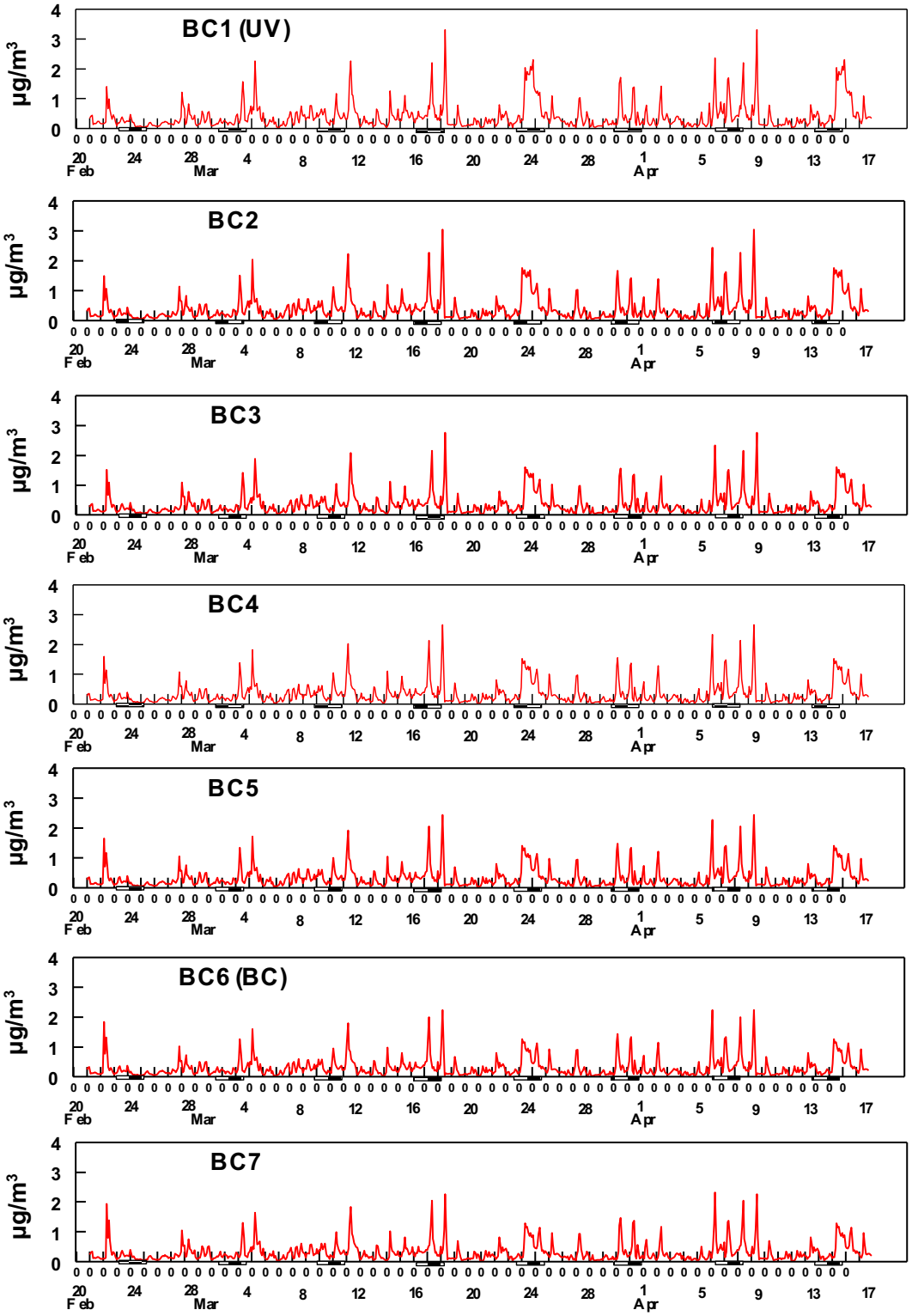

Figure 3. Two-hour average data for the 7 channel aethalometer. The hash marks under the X axis indicate weekends.

While CO was used in the initial PMF analyses for both dichloromethane and $PM_{2.5}$, examination of the data for CO in Figure 2 suggested that the base line for the measurement was variable for the data set and an examination was made of the effect of removing CO from the PMF analyses. The result was about a 30% improvement in the goodness of fit for both analyses. CO was therefore not included in the final PMF analyses for either dichloromethane or $PM_{2.5}$.

The values used to create the U matrix for the data in Figures 2 and 3 are given in Table 2

Table 2. Values used in the creation of the uncertainty matrix for PMF analysis of the species in Figures 2 and 3. The units for NO_X is ppb and for the AE data $\mu g/m^3$.

Value	NO_X	AE Channel						
		1	2	3	4	5	6	7
LOD	2.0	0.05	0.05	0.05	0.05	0.05	0.05	0.05
Precision	0.10	0.10	0.10	0.10	0.10	0.10	0.10	0.10

The following data were available for the PMF evaluation of the sources of $PM_{2.5}$.

1. Data used in both dichloromethane and $PM_{2.5}$ analyses. This included the data given in Figures 2 and 3 with the accompanying data in Table 2.
2. Data measured with the OAM. This included levoglucosan, fluorene, pyrene, stearic acid and anthracene. These data are shown in Figure 4 and the values used in the creation of the U matrix for these species is given in Table 3.

Table 3. Values used in the creation of the uncertainty matrix for PMF analysis of the species in Figure 4. Units for the data are peak area.

Value	Levoglucosan	Fluorene	Pyrene	Stearic Acid	Anthracene
LOD	1.0	0.02	0.02	0.02	0.80
Precision	0.20	0.20	0.20	0.20	0.20

A comment should be made about the precision values for the compounds measured by the OAM shown in Table 3. In our two previously reported PMF analyses using OAM data (Cropper et al. 2018, 2019) the value used for the precision of the OAM measured compounds was 8%. However, an unintended variation in the start time of the instrument in this study gave added variability to these measurements. The response of the PMF analysis using the set of compounds listed in Table 3 was not as expected. It was therefore assumed that the precision of the data was higher than expected and a value of 20% was tried in the PMF analysis. The change

improved the goodness of fit by a factor of almost 4 (21095 to 5459). It should be noted that the degrees of freedom for the data set was 6146. Therefore, the precision values given in Table 3 were used in the final $PM_{2.5}$ PMF analysis.

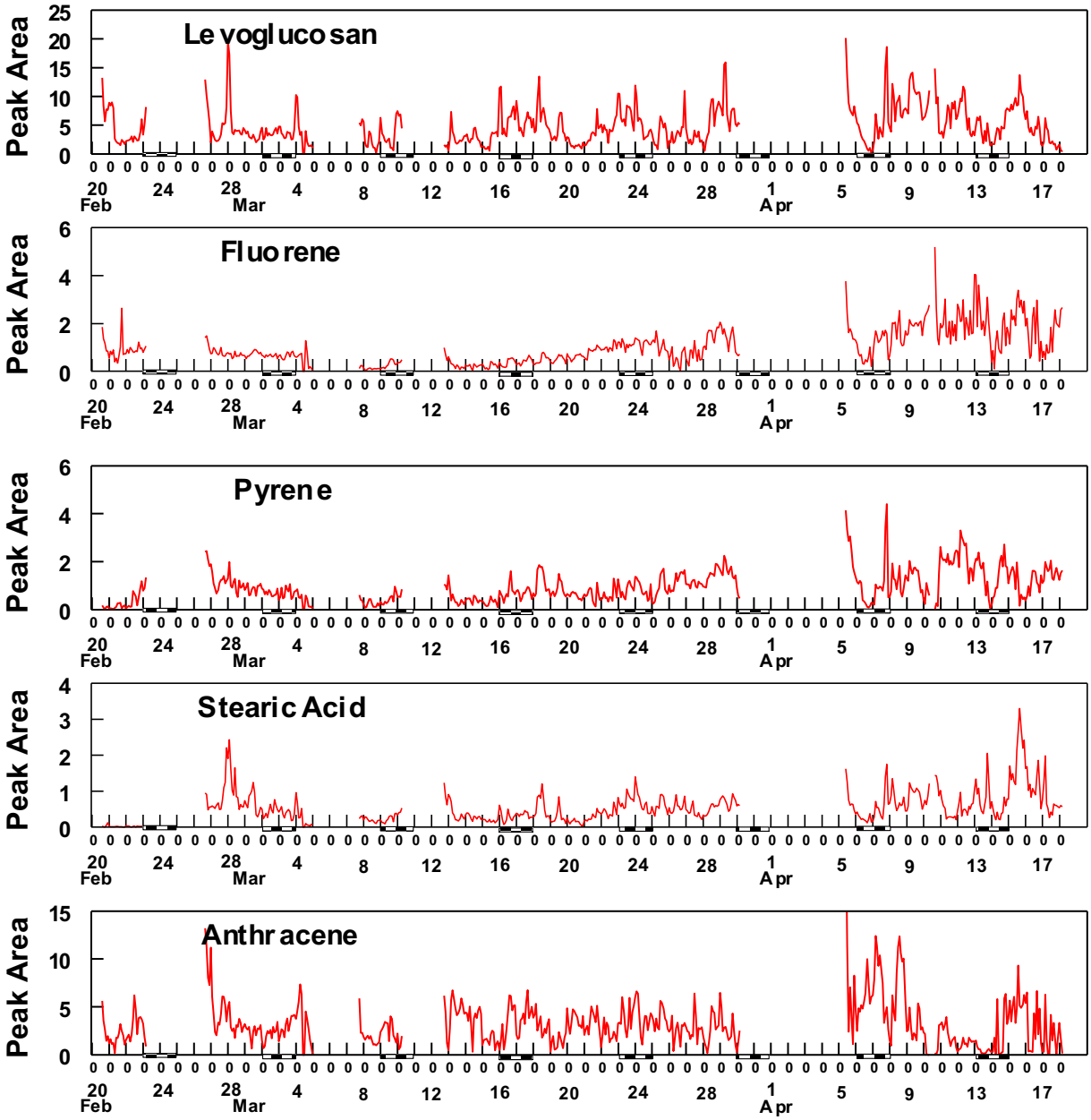

Figure 4. Two-hour average data for the OAM measured compounds. The hash marks under the X axis indicate weekends.

5. Results of the PMF Analyses

While the main objective of the PMF analysis was the apportionment of sources of dichloromethane, the results of the $PM_{2.5}$ PMF analysis provided insights into the

dichloromethane PMF analysis, thus the $PM_{2.5}$ analysis results will be presented first.

6. Apportionment of Sources of $PM_{2.5}$

EPA-PMF v5.0 analysis was conducted by incrementally assuming 2 to 5 factors as solutions. It was recognized that not all of the measured $PM_{2.5}$ would be described by the analysis since the input species ($PM_{2.5}$ and the species in Figures 2 (excluding CO), 3 and 4) contain only $PM_{2.5}$ components that are related to primary emissions of fine particulate material. There were no components which would allow for the identification of secondary species such as ammonium nitrate or secondary organic material. As expected, a large fraction of the fine particulate material was not accounted for in each solution. However, the solutions became more reasonable in moving from 2 to 3 factors but did not improve for 4 or 5. An evaluation of the quality of the fitted data can be obtained by comparing the degrees of freedom (i.e. the number of data points) with the calculated value of *Q* (goodness of fit parameter, EPA 2014). If a reasonable fit is obtained, the calculated value of *Q* should be equal to or less than the degrees of freedom. A Q value greater than the degrees of freedom value suggests that the errors in the model are not well defined. For this analysis the degrees of freedom (14 parameters and 493 data sets) were 6902. Three factors were taken to be the optimal solution. For the base analysis with three factors the Q value was 5459. The three factors were found to correspond to emissions from wood burning, diesel traffic and auto traffic. The diel patterns for the $PM_{2.5}$ for the three-factor solution resulting from applying constraints to the base analysis for these three factors shown in Figure 5. The constraints applied were to minimize the presence of levoglucosan in the diesel and auto factors and to minimize the presence of the aethalometer data in the auto factor. This solution resulted in a Q value of 5550 with the profiles of the various factors as given in Table 4. As noted in Table 4, not all the levoglucosan could be constrained to be in only the Wood Smoke Factor. If the contribution of levoglucosan in the Auto Emissions Factor was forced to zero, that factor would disappear. This is probably due to the small amount of material in the Auto Emission Factor. It should be noted, however, that the other marker compound which should be associated with wood smoke, stearic acid, is also found in the Wood Smoke Factor without constraint on this species.

As noted in Table 4, 2.29 $\mu g/m^3$ of the $PM_{2.5}$ (62%) was not accounted for in the PMF analysis. This is expected as secondary material cannot be accounted for in this analysis. This material not accounted for can be further broken down into two different fractions. Both of our previous two publications using OAM measured marker compounds in a source apportionment where the secondary material could be accounted for (Cropper et al, 2018, 2019) have shown that in addition to the presence of primary wood smoke particles associated with the emissions from burning of wood, secondary organic material is also formed from the gas phase chemistry of wood smoked emitted gases. This secondary wood smoke material was observed concurrent with the primary wood smoke particulate emission and at about the same concentration as observed for the primary particulate emissions. The results of the PMF analysis reported here show that this same chemistry may be postulated to occur in this study. Figure 6 compares the measured concentrations of $PM_{2.5}$, the $PM_{2.5}$ not accounted for in the PMF analysis and the concentrations of the Wood Smoke Factor.

Table 4. Profile of the final $PM_{2.5}$ PMF three factor solution.

Total Average $PM_{2.5}$	3.68 μg/m^3		
Total $PM_{2.5}$ in Factors	1.39 μg/m^3		
$PM_{2.5}$ not fit	2.29 μg/m^3		
Factor	Wood Smoke	Diesel Emission	Auto Emissions
$PM_{2.5}$ in Factor	0.97 μg/m^3	0.46 μg/m^3	0.05 μg/m^3
% Levoglucosan	68	0	32
% Fluorene	0	6	93
% Pyrene	11	7	81
% Stearic Acid	80	0	20
% Anthracene	74	9	16
% BC1	12	87	1.0
% BC2	13	86	0.9
% BC3	14	85	0.3
% BC4	15	85	0.1
% BC5	16	84	0
% BC6	17	83	0
% BC7	17	83	0
% NO_X	53	47	0
Secondary Wood $PM_{2.5}$	0.77 μg/m^3		
Other PM	1.63 μg/m^3		

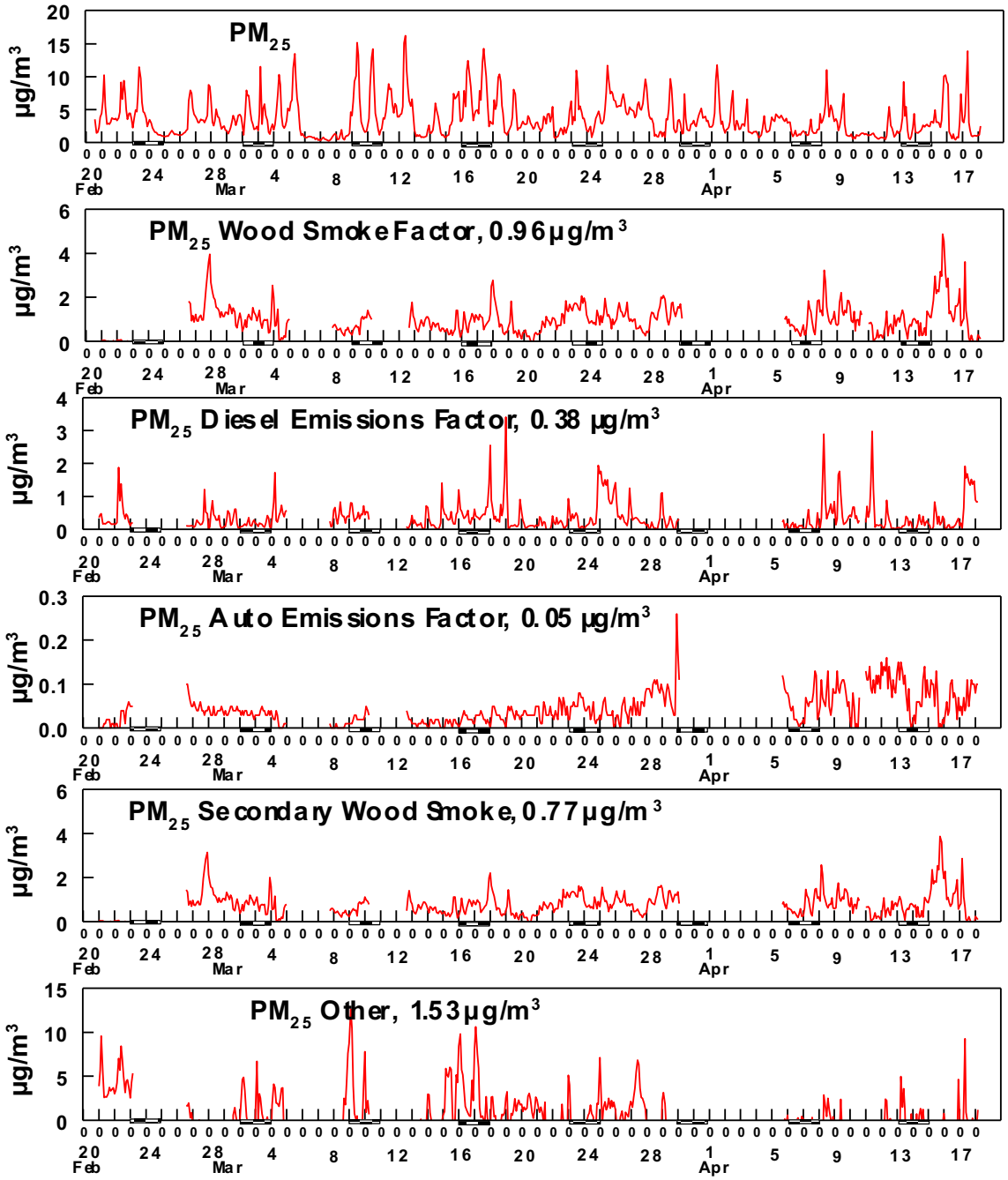

Figure 5. Diel patterns for measured $PM_{2.5}$, the three factors identified in the PMF analysis and assignment of the remaining unidentified mass into two classes, see text. The hash marks under the X axis indicate weekends.

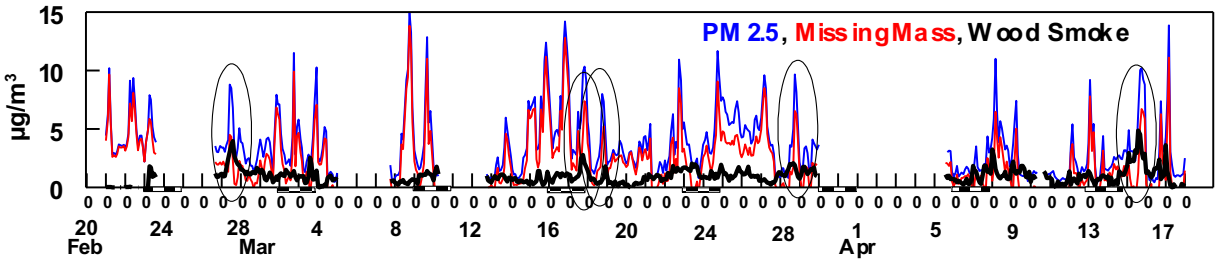

Figure 6. Comparison of the measured concentrations of $PM_{2.5}$, the $PM_{2.5}$ not accounted for in the PMF analysis and the concentrations of the Wood Smoke Factor. The hash marks under the X axis indicate weekends.

There are several periods in the data when concurring peaks are seen in the missing mass and wood smoke data shown in Figure 6. The elliptical circles in Figures 6 highlights the more prominent occurrences. It seems reasonable, based on our previous observations (Cropper et al., 2018, 2019) to postulate these are due to secondary aerosol formed from gases emitted during the combustion of wood. The estimation of the ratio of primary to secondary wood smoke is difficult because of the lack of direct apportionment of secondary material in this study, the possible presence of other sources during the time periods highlighted and the uncertainty of where base lines for the observed peaks should be drawn. However, if we assume this ratio is roughly constant, as was observed in our previous studies, the best estimate of the ratio may be made for the data on February 27. Integration of these data with the estimate that the wood smoke factor data identify a reasonable base line give a ratio of secondary to primary wood smoke aerosol of 0.79. This gives the diel pattern for the estimated concentrations of secondary wood smoke aerosol shown in Figure 5. The remaining aerosol is labeled $PM_{2.5}$ Other in Figure 5. This last category will be due to secondary aerosols such as ammonium sulfate or ammonium nitrate. A pie chart of the aerosol composition based on this analysis is shown in Figure 7. These results are consistent with results published by Kotchenruther (Kotchenruther, 2016).

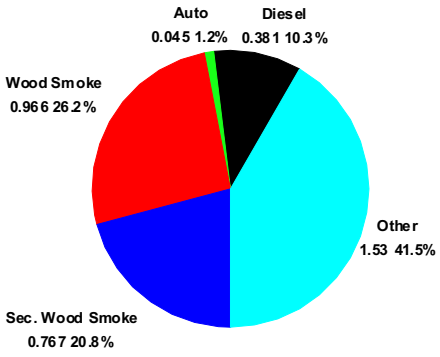

Figure 7. Pie chart of the $PM_{2.5}$ composition based on analysis of the PMF results.

7. Apportionment of Sources of Dichloromethane

EPA-PMF v5.0 analysis was conducted by incrementally assuming 2 to 5 factors as solutions. It was recognized that not all of the measured dichloromethane would be described by the analysis since the input species (dichloromethane and the species in Figures 1, 2 (excluding CO), and 3 plus $PM_{2.5}$ would allow for the attribution of some dichloromethane but not the dichloromethane which was not associated with any of the other species. Analysis using these species indicated that as we increased from 2 to 3 or 4 factors the NO_X and $PM_{2.5}$ became associated with factors with little or no dichloromethane, indicating they were not species which should be included in the analysis. Therefore, these two species were deleted from the PMF analysis. The resulting final analysis gave two factors, one of which contained all the species in Figure 1 and one of which contained all the species in Figure 3. These were assumed to represent contributions of dichloromethane from the refinery emissions and from diesel traffic emission, respectively based on their association with the BTEX and aethalometer data, respectively as shown in Table 5. The final PMF analysis for dichloromethane contained 12 components and 443 data sets (5316 degrees of freedom). The Q values for the base fit was 2942. Constraint analysis was applied to maximize the respective sets of contribution to each factor. The resulting Q values for the constrained fit was 2968. The final result contained two factors as shown in Table 5 and Figure 8.

Table 5. Profile of the final dichloromethane PMF two factor solution.

Total Average DCM	0.345 ppb	
Total DCM in Factors	0.058 ppb	
DCM not fit	0.287 ppb	
Factor	Refinery	Diesel Emissions
DCM in Factor	0.052 ppb	0.006 ppb
% Benzene	96	4
% Toluene	93	7
% Ethylbenzene	100	0
% Xylene	89	11
% BC1	0	100
% BC2	0	100
% BC3	0	100

% BC4	0	100
% BC5	0	100
% BC6	0	100
% BC7	0	100

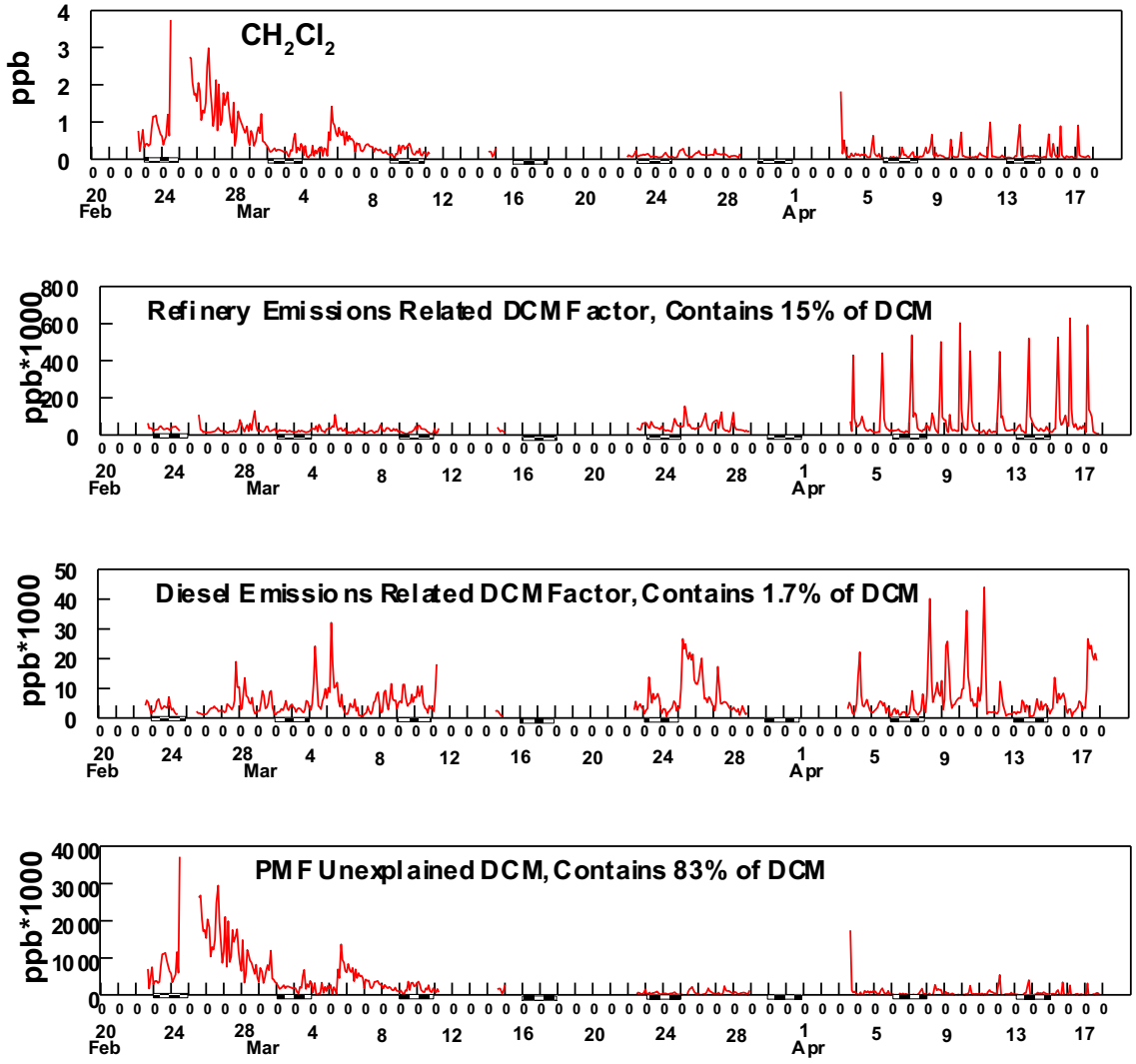

Figure 8. Diel patterns for measured dichlromethane, the two factors identified in the PMF analysis and the PMF unexplained dichloromethane. The hash marks under the X axis indicate weekends.

As indicated, one of the factors in the dichloromethane PMF analysis was assumed to be associated with emissions from diesel traffic. As outlined above, the $PM_{2.5}$ PMF analysis results in a PM Diesel emissions related factor. These two independent solutions are compared in

Figure 9. It should be pointed out that these two analyses included different numbers of data sets and different time periods. However, where the two results overlapped the agreement between the two independent analyses is evident. This provides strong support for the association of 1.7% of the dichloromethane with emissions from diesel traffic.

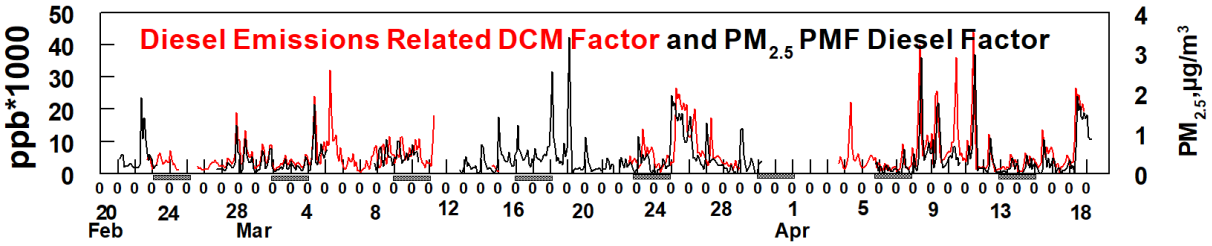

Figure 9. Comparison of the Diesel Emissions Related DCM Factor and the $PM_{2.5}$ PMF Diesel Factor. The left Y axis is for dichloromethane and the right Y axis is for $PM_{2.5}$. The hash marks under the X axis indicate weekends.

A pie chart of the sources of dichloromethane based on this analysis is shown in Figure 10.

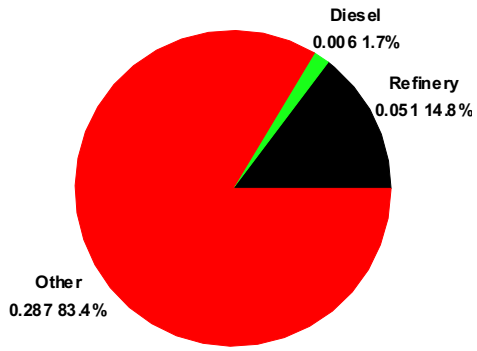

Figure 10. Pie chart of the sources of dichloromethane based on the PMF analysis.

While the origins of the other factor,the dichloromethane not accounted for in the PMF analysis, are not as clearly identified as for the dichloromethane associated with the Diesel Emissions Related DCM Factor in the analysis reported here, the results do give some indication of probable sources. The diel patterns suggest that the Refinery Related DCM Factor and the PMF Unexplained DCM represent inputs of dichloromethane under quite different meteorological conditions. The Refinery Related DCM Factor is so identified based on the observation that the set of compounds associated with this factor are those expected to be emitted from an oil refinery. These are located to the west and south of the sampling site. The suggested sources should be further confirmed by comparison of the results in Figure 8 with meteorological back-trajectory data. This is done in Section 9.

8. Formaldehyde Source Apportionment

Formaldehyde is both a primary and a secondary formation species. As described in the report on the PMF analyses done on both dichloromethane and $PM_{2.5}$, the species that were used in

these PMF analyses all involve primary emitted species. Secondary species such as particulate nitrate, sulfate or secondary organic material were not available from the results of the study and secondary material related factors could not be identified. As a result, a substantial fraction of the dichloromethane or $PM_{2.5}$ was not identified in the PMF analysis. This unidentified material was interpreted as primary emitted dichloromethane or secondary fine particulate matter.

Formaldehyde has both primary and secondary sources in the atmosphere. Secondary gas phase CH_2O is formed from free radical reactions with a wide variety of gas phase organic molecules. Most secondary formation is expected to be formed from the photo-oxidation of ethene, propene and larger terminal alkenes, but CH_2O is also formed, albeit more slowly, from the oxidation of alkanes and aromatic compounds. The principal way that a PMF analysis of the Bountiful data could provide information on the formation of formaldehyde would be if the limited gas phase species included in the data set were the dominant precursor to the formation of formaldehyde. The set of compounds which have been attributed to refinery emissions would need to be involved in this analysis.

Figure 11 compares the diel patterns of benzene, one of the set of refinery associated compounds and measured formaldehyde. As the refinery associated gases are all highly correlated, similar results would be obtained using any of the other species in the data set.

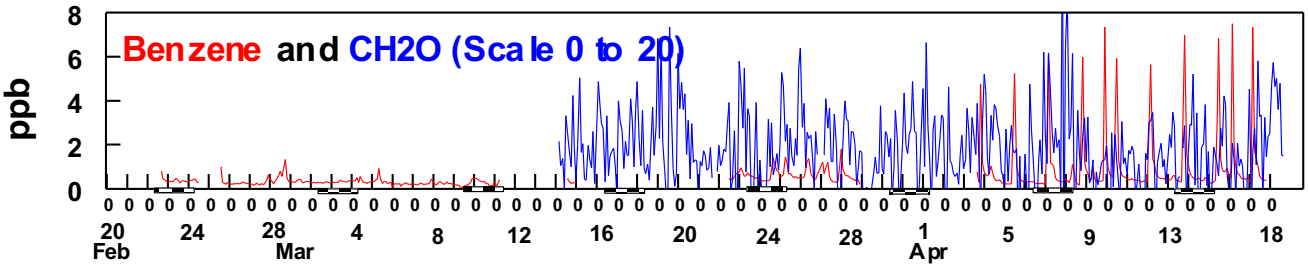

Figure 11. Comparison of the measured concentrations of benzene and CH_2O. The hash marks under the X axis indicate weekends.

Fairly complete results for formaldehyde are available from 15 March through 15 June although for visualization purposes only data from March through April is included in Figure 11. The time period when high concentrations of refinery emitted gases are present is the April 3 through April 18 time period (Figure 12). If benzene (or any of the other VOCs measured during this study including ethylbenzene, toluene, or xylenes) were closly linked to formation of formaldehyde then, during the daylight hours a formaldehyde peak should lag behind the benzene peak. The time lag between a peak in BTEX and the formation of CH_2O is dependent on the atmospheric oxidation reaction rates that convert hydrocarbons into CH_2O and are dependent on the ambient temperature, solar flux, and concentrations of species such as NO_x. The time period from April 3 through April 18 is shown in Figure 12.

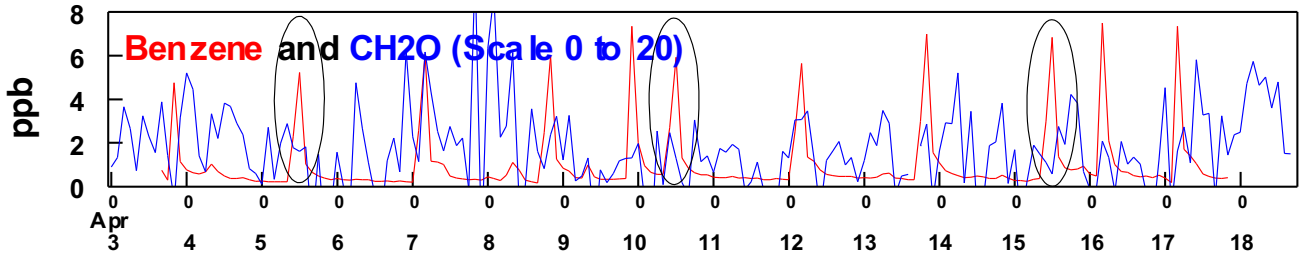

Figure 12. Comparison of the measured concentrations of benzene and CH_2O for the time period April 3 through April18. The hash marks under the X axis indicate weekends.

Previous work has shown that upwards of 16% of the CH_2O concentrations measured in the Salt Lake Valley can be attributed to the refineries (Jaramillo et al. 2020). If the formation of formaldehyde was dominated by refinery emitted BTEX then we would expect the appearance of a formaldehyde peak to consistenly follow the appearance of a day-time benzene peak (illustrated by the ovals in Figure 12), with minimal occurrence of formaldehyde at other times. This relationship is not observed nor is it expected because of the highly variable and slow atmospheric oxidation rate that converts species like BTEX into CH_2O. This is further validated by Figure 13 which shows the same data as Figure 12 but with a 3 hour lag to the left so that the benzene peak and the formaldehyde peak should overlap if the formation of formaldehyde is driven by the presence of the refinery emitted BTEX. While there are three occasions when this may be true (illustrated by the ovals in the graph), the formation of formaldehyde is clearly not dominated by the presence of the refinery emited BTEX. However, there is a relationship observed between O_3 and CH_2O at the Bountiful site.

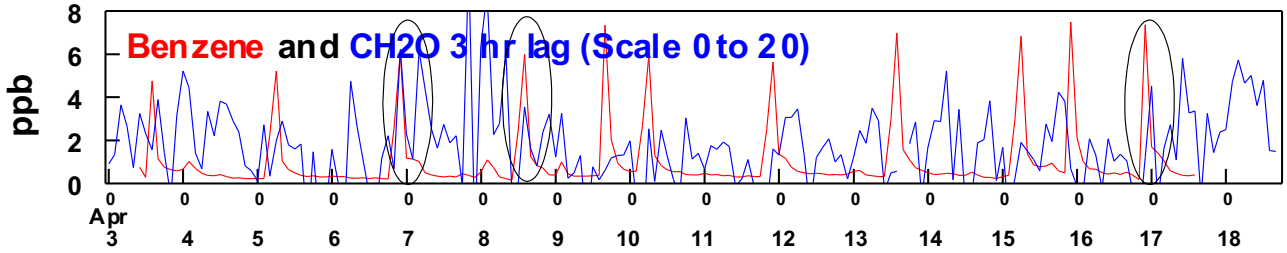

Figure 13. Comparison of the measured concentrations of benzene and CH_2O (with a three-hour lag in the CH_2O data) for the time period April 3 through April 18.

8.1 Relationship Between O_3 and CH_2O

The mechanism that is primarily responsible for the production of trophospheric ozone is similiar to the mechanism that produces CH_2O and involves the photo-oxidation of hydrocarbons in the presence of NO_x. Rections 1-5 define the mechanism for production of trophospherie O_3 from any hydrocarbon (RH).

$$\mathbf{RH + \cdot OH \rightarrow R\cdot + H_2O} \quad (1)$$

$$\mathbf{R\cdot + O_2 \rightarrow RO_2\cdot} \quad (2)$$

$$\mathbf{RO_2\cdot + NO \rightarrow NO_2 + RO\cdot} \quad (3)$$

$NO_2 + h\nu \rightarrow NO + O$ (4)
$O + O_2 \rightarrow O_3$ (5)

Reactions 6-9 describe the mechanism for production of CH_2O from the photo-oxidation of C_2H_2 (ethylene), frequently the highest concentration VOC emitted by a refinery, but can be generalized to any hydrocarbon, RH.

C_2H_2 (RH) + ·OH → $HOCH_2CH_2$ (R·) (6)
$HOCH_2CH_2$ (R·) + O_2 → $HOCH_2CH_2O_2$ (RO_2·) (7)
$HOCH_2CH_2O_2$ (RO_2·) + NO → $HOCH_2CH_2O$ (RO·) + NO_2 (8)
$HOCH_2CH_2O$ (RO·) + O_2 → HO_2· + 2 CH_2O (9)

The reactions highlighted in black are the same in the two mechanisms. If the hydrocarbon that is being photo-oxidized is something other than C_2H_2, for example BTEX, the mechanism that describes the oxidation has several additional reactions that delay the formation of CH_2O. However, because of the relative high concentration of hydrocarbons that are typically emitted by refineries and react in a similar fashion as to what produces tropospheric ozone it is expected that a correlation between O_3 and CH_2O may be observed. Figure 14 shows the relationship between measured concentrations of O_3 and CH_2O at the Bountiful sampling site for the months of April, May and June (2019).

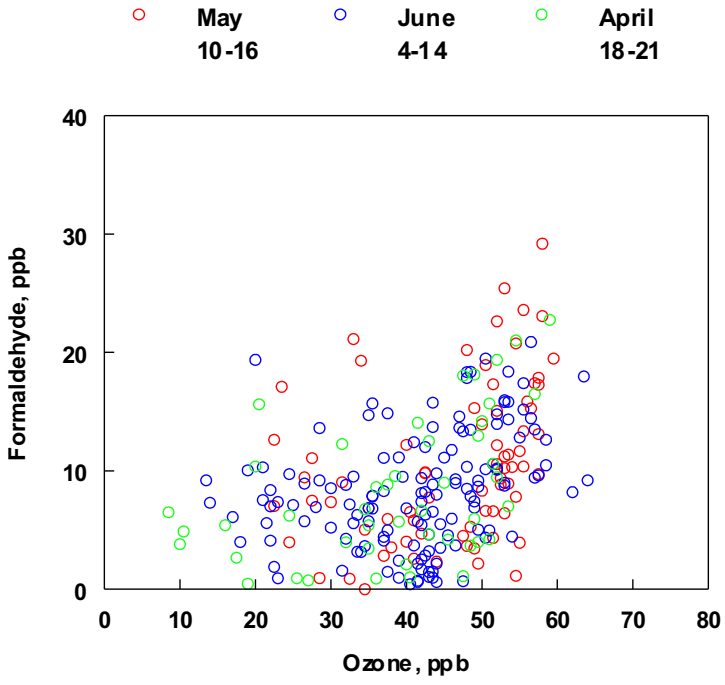

Figure 14. Comparison of the concentrations of ozone and formaldehyde for the three indicated time periods.

The data was futher constrained by plotting O_3 and CH_2O concentrations when the wind was blowing between 190-220° and between the hours of 8 am – 6 pm. (A wind direction of between

190 and 220° encompasses the range of oil refineries located to the south southwest of the Bountiful air sampling site). Figure 15 shows this relationship.

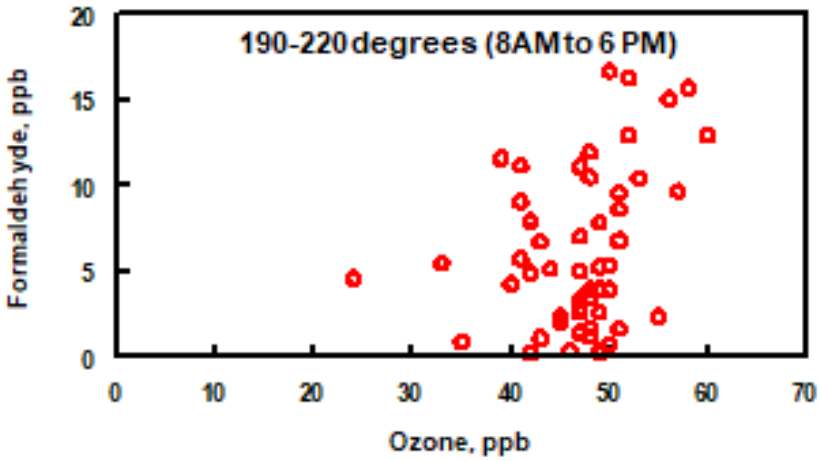

Figure 15. Comparison of ozone and formaldehyde concentrations between the indicated wind direction and time period.

Figure 15 suggests a correlation between O_3 and CH_2O during the daytime when the wind is blowing from the south southwest. For comparison purposes, Figure 16 shows a plot of O_3 verses CH_2O during daytime when the wind is blowing from between 260-290° (north, northwest).

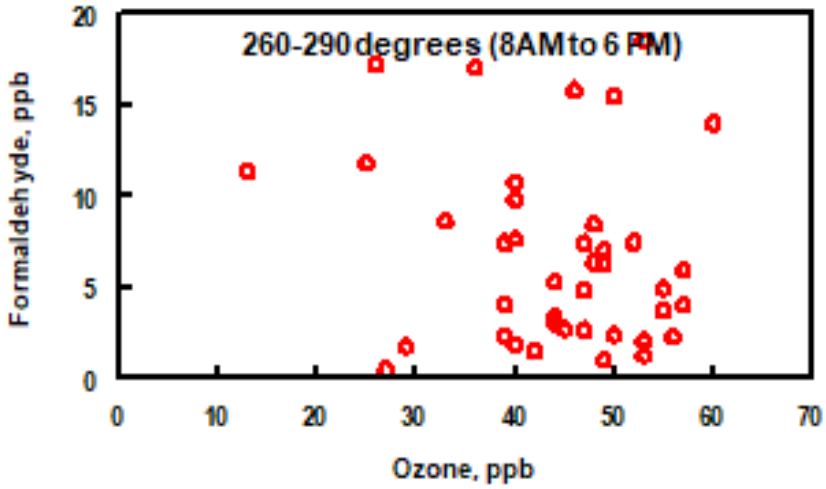

Figure 16. Comparison of ozone and formaldehyde concentrations between the indicated wind direction and time period.

When the wind is blowing from the north, northwest towards the sampling site the correlation between O_3 and CH_2O is not as pronounced as when the wind is blowing from the south, southwest.

Examination of Figure 17 (blue trace) shows that frequently the peak in CH_2O matches the peak in the actinic flux. The peak in CH_2O is often observed between 12:00-14:00 hours when photochemical production of OH radical, driving the photooxidation of VOC's and production of CH_2O, is at a maxium. This is consistent with the diurnal patten of CH_2O that typically shows a peak in its formation during daylight hours (Figure 17). This relationship indicates that CH_2O is primarily a secondarily formed pollutant.

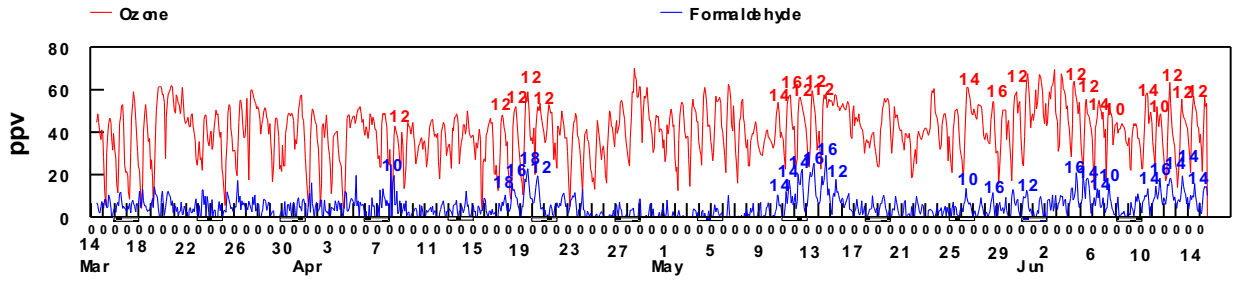

Figure 17. Comparison of O_3 and CH_2O concentrations between March 14 and June 14. The hour of the day in which O_3 and CH_2O peak are labeled for some of the observed peaks.

Since the formation of formaldehyde is associated with the presence of the refinery emitted gases as seen in Figures 14, 15 and 16, but not strongly correlated to BTEX emissions, the source apportionment of formadehyde is not possible in a PMF analysis of the data. The data, however, may provide valuable input for chemical reaction modeling.

9. Correlation Between the PMF Results for the Dichloromethane Refinery Related Factor and the Back-Trajectory Data for the April data

The Refinery Related DCM Factor is so identified based on the observation that the set of compounds associated with this factor are those expected to be emitted from an oil refinery. The diel patterns for the observed BTEX is such that the source must be operating continuously, thus sources such as automodile exhausts, auto shops or other business using paints and coating are unlikely to be the dominate source of the observed BTEX. Refineries are located to the west and south of the sampling site. However, it is worth noting that other sources such as filling stations, automotive exhaust, and paints and coatings can contribute to BTEX, and these source types are also located in proximity to the refineries. Previous canister measurements made by the State of Utah show the consistent presence of chloromethane, dichloromethane, chloroform, and carbon tetrachloride. These species are expected to be formed concurrently from the reaction of methane gas with chlorine, as can be expected to occur in refinrery operations. The suggested refinery souce should be further confirmed by comparison of the results in Figure 8 with meteorological back-trajectory data.

The pertinent time period from the referenced Figure 8 for the occurrence of the refinery associated dichloromethane factor is the April 3 through April 18 period when this factor was present at other than minimal concentratons. There were a total of 11 prominent peaks in the factor concentration as shown in Figure 18. The start of the 2 hour time period for the maximum dichloromethane concentration in each peak is given above the peak.

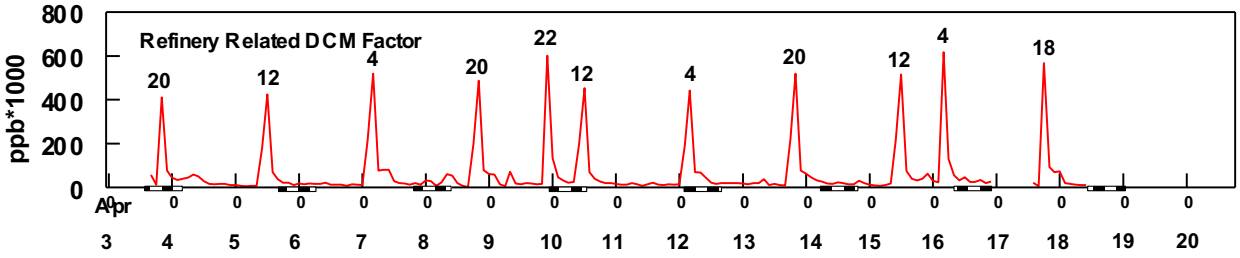

Figure 18. Diel pattern for the refinery associated dichloromethane factor and the start time for the maximum of each observed peak. Hash marker under the X-axis indicate weekends.

Two figures follow (combined as Figure 19) which provide insights into the source strengths of the oil refineries near Bountiful and the transport path from those refineries to the sampling site. There may be other sources in this transport path which make 24 hr contributions to BTEX. We do not have data on refinery-related emissions of the aromatic compounds measured in the Bountiful study, but if we assume they are related to the number of barrels of oil processed each day as given in the figure caption, then the refineries will contribute as sources of BTEX and dichloromethane to the Refinery factor in proportion to the number of barrels of oil they process. The second graph shows the shortest path from the sample site for the Bountiful study to the Tesoro refinery. The distance is only 9 miles and if emissions from the refineries were to impact the Bountiful site, it would require a transport path from the refinery north to the sampling site. To test this possibility, the back-trajcetory data corresponding to each peak in Figure 18 are displayed in Figure 20.

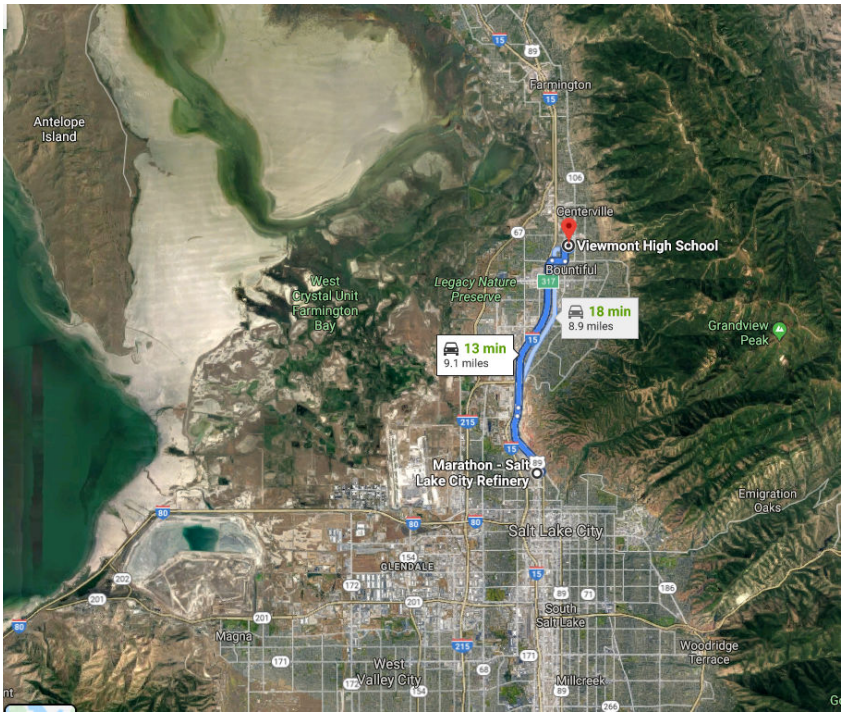

Figure 19. The top portion is from Cropper et al, 2019 and indicates the locations of the various oil refineries to the south of the Bountiful sampling site. The corresponding barrels of oil processed each day are Holly (39.3K), Silver Eagle (15K), Chevron (54.7K), Big West (30.5K) and Tesoro (61K). The bottom portion indicates the distance between the sampling site and the Tesoro refinery.

There are a few points to consider in evaluating the comparisons shown in Figure 20. First, we should recognize that the identification of the approach to the sampling site of emissions from the refineries by the back-trajectory model is challenging because of the short transport distance. Second, we should recognize that not every back-trajectory that approaches the sampling site from the south will be associated with an impact of emissions from the refineries, again because of the short transport distance, and the presence of other potential primary and secondary sources in the area.

As indicated in Figure 20, the long distance back-trajectories associated with each factor peak concentrations come from northerly, western and southerly directions. However, in all cases but one (the trajectory with an oval around it), the approach of the trajectory to the sampling site is well defined as being from the south. Also, in most cases, the turn in that trajectory to give that approach from the south is not much longer than a few times the distance from the sampling site to the refineries. The hypothesis that this factor identified in the PMF analysis is associated with emissions from the refineries is strongly supported by the back-trajectory data. However, recommendations are provided in section 12 of this report that if followed will provided additional clarifying data about this hypothesis.

It should be pointed out that the great variability of the endpoints of the back trajectories shown in Figure 20, and the short distance of the refineries from the sampling site indicate that a probability analysis of these data would not be useful.

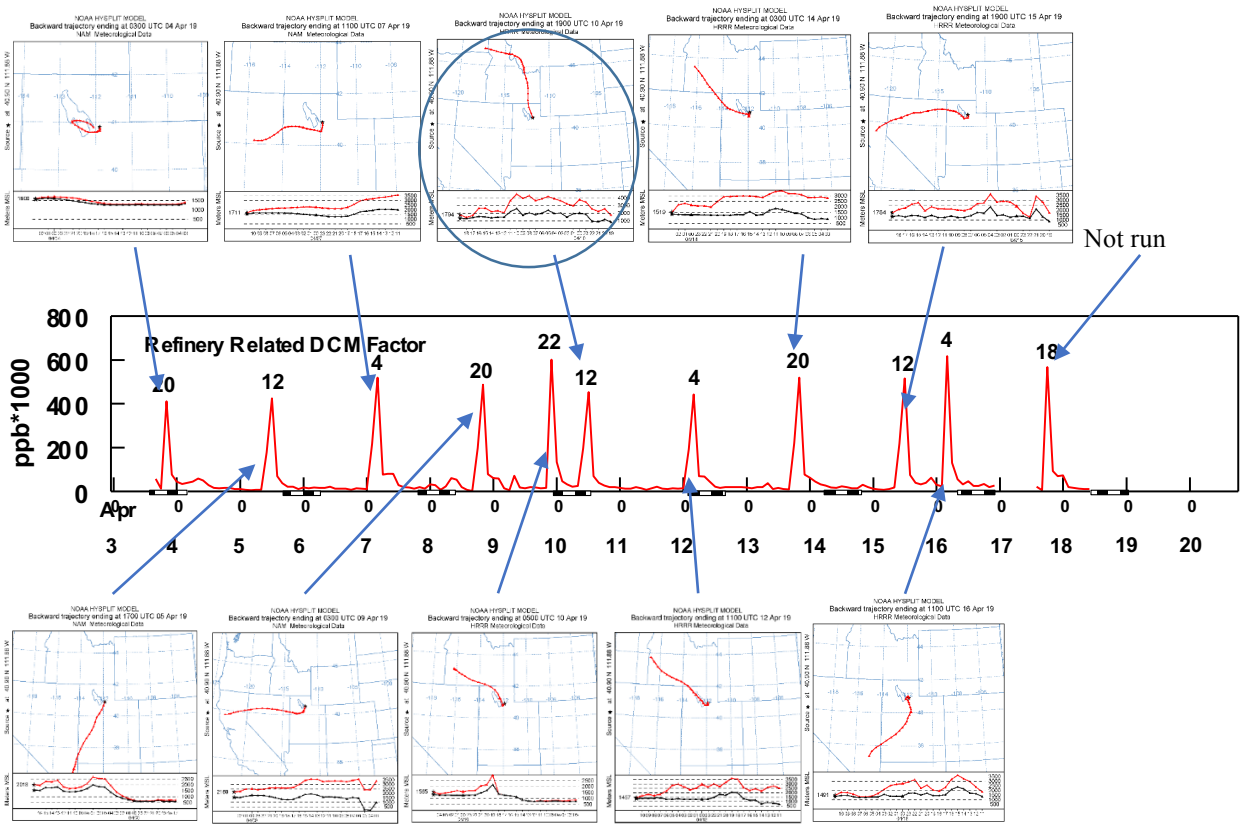

Figure 20. Combination of the diel pattern for the refinery associated dichloromethane factor and the back-trajectory corresponing to each identified peak in that diel pattern.

10. Correlation Between the PMF Results for the Dichloromethane Refinery Related Factor and the Back-Trajectory Data for the February and March data

The results of the original PMF ananlysis for the "Refinery Related DCM Factor" and for the unexplained dichloromethane in the PMF analysis is shown in Figure 21.

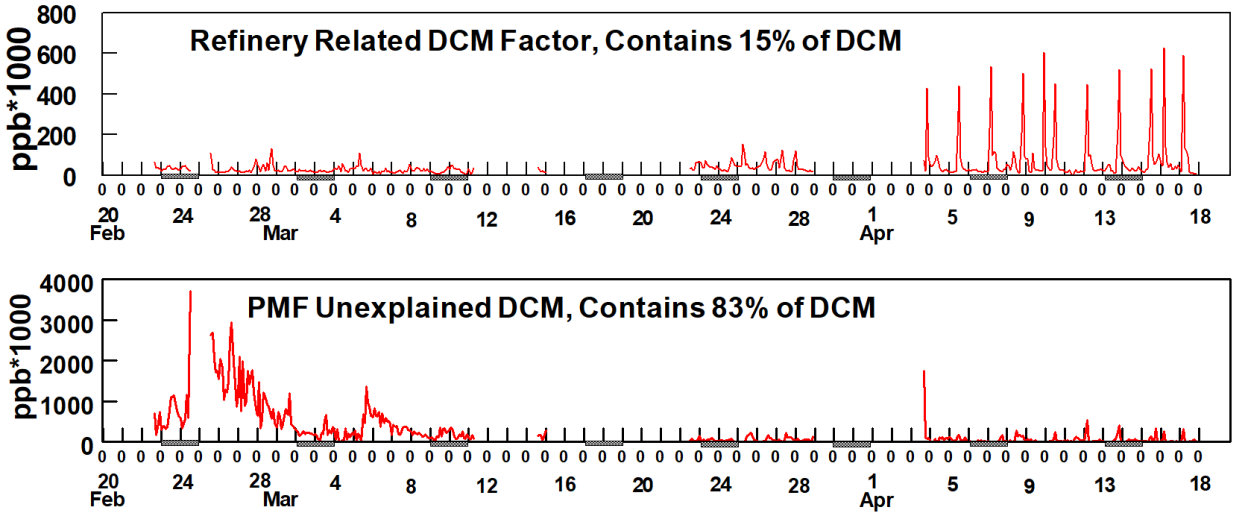

Figure 21. Diel pattern for the Refinery Related DCM Factor and PMF Unexplained DCM in the original PMF analysis using all data.

10.1 Reconsideration of the February – March PMF Results

The original PMF analysis indicated that the Refinery Related DCM factor was present at much lower concentrations during February and March than during April in the original PMF analysis including all of the the data, Figure 21. However, initial examination of the correlation between the peaks in the dichloromethane concentrations during the April time period and the same correlation in the February – March time period indicated similar results, i.e. that a DCM Factor associated with BTEX was present in both time periods. It is puzzling that the concentrations in February and March were so low compared to those seen in April, although they appear to be from the same source, both being related to BTEX. It is possible that a difference in atmospheric mixing heights during Feburary-March compared to April are responsible for the difference in DCM concentrations. Another possible reason for this observation may be that the PMF Unexplained DCM was minimal during the April time period, but much higher than the concentrations of the Refinery Related Factor during February and March. It is reasonable that this could be a result of the difference in the fit between the two time periods being effected by the differences seen in Figure 21 in the relative concentrations of these two species for the February – March compared to the April time period. Therefore, to focus on the February – March time period, a second PMF analysis was done on the data set, but using only the February and April data in this reanalysis. The results of the two analyses for the February – March time period using all data and using only the January – February data are shown in Figure 22.

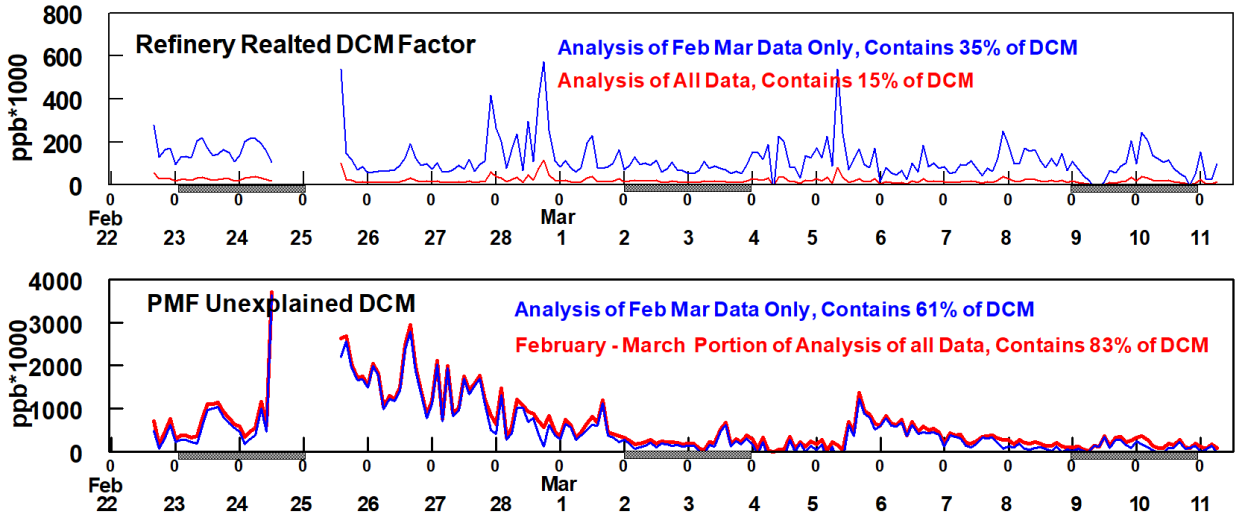

Figure 22. Diel pattern for the Refinery Related DCM Factor and PMF Unexplained DCM during February and March in the original PMF analysis using all data compared to that obtained for analysis of only the February and March data.

The assignment of the total dichlromethane to each of the components in the two PMF analyses is given in Table 6.

Table 6. Distribution of the dichloromethane between the two PMF factors and the unexplained dichloromethane for the two analyses.

Analysis	DCM Total, ppb	DCM Refinery Factor, ppb	DCM Diesel Factor, ppb	PMF Unexplained DCM, ppb
All Data	0.334	0.051	0.006	0.287
February-March	0.334	0.121	0.012	0.197

As noted in Figure 22 and Table 6 the difference in the two PMF analysis has the major effect of shifting proportioned dichloromethane during the February – March time period such that the magnitude of the dichloromethane peaks seen in February and March, Figure 22, is more comparable to the magnitude seen in April, Figure 21. We have taken the blue line results in Figure 22 to be a better data set for the comparison of the PMF results to the back trajectory data for February and March. The main difference in the patterns of the dichloromethane during the two time periods is there are more frequent high peaks in April, but an overall higher baseline to the data in February and March.

10.2 Correlation with the Refinery Associated PMF Factor

There are a few points to consider in evaluating the comparisons shown in Figure 23. First, we should recognize that the identification of the approach to the sampling site from a refinery by the back-trajectory model is challenging because we are looking at a very short transport distance. Second, we should recognize that not every back-trajectory that approaches the

sampling site from the south will be associated with an impact of emissions from the refineries, again because of the short transport distance and the presence of other potential sources in the area.

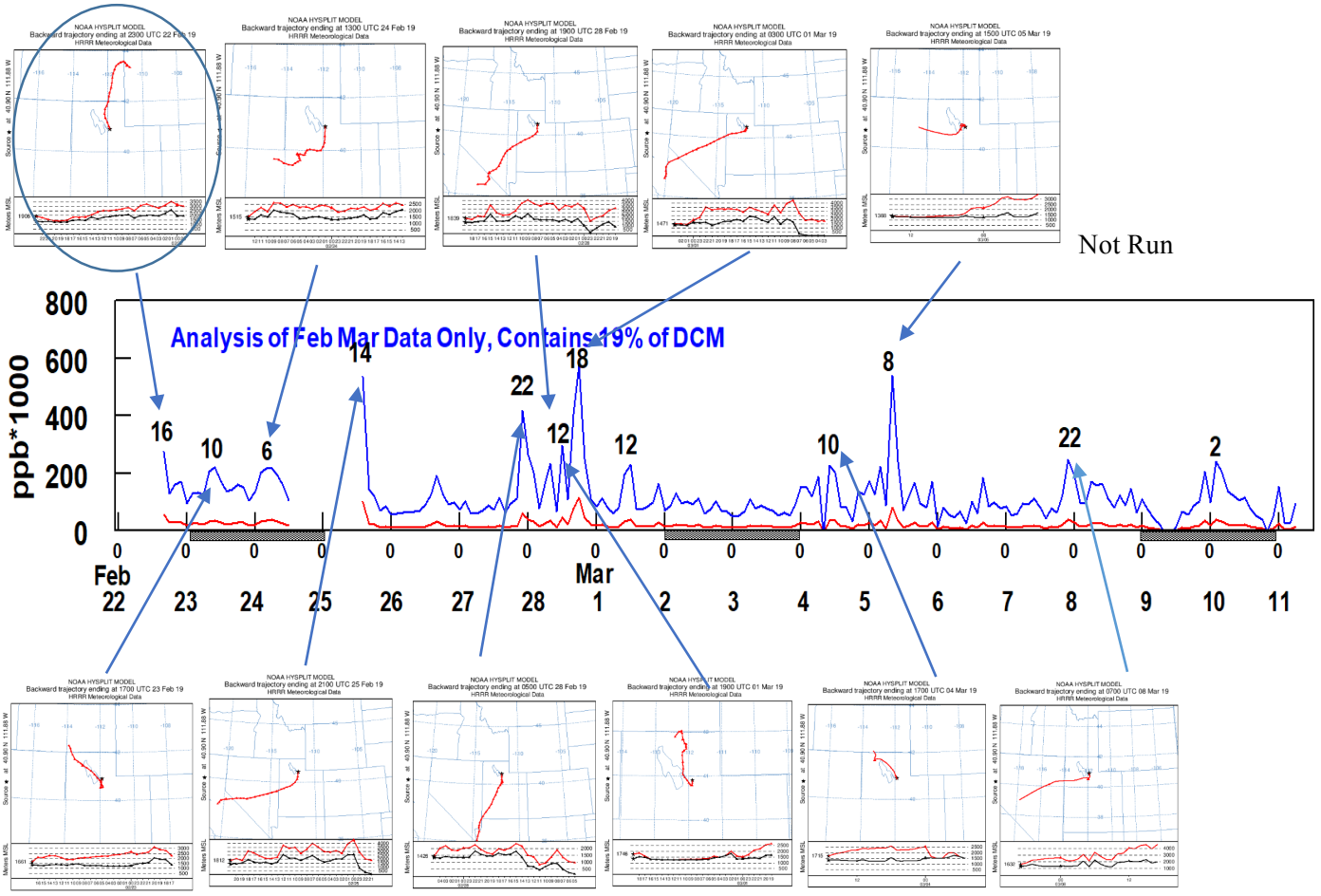

Figure 23. Comparison of the diel pattern for the refinery associated dichloromethane factor and the back-trajectory corresponing to each identified peak over 200 in that diel pattern. The red line in the diel plot is the concentration predicted by PMF ananlysis of all the data.

As indicated in Figure 23, the long distance back-trajectories associated with each factor peak concentrations come from northerly, western and southerly directions. However, in all cases but one (the trajectory with an oval around it) the approach of the trajectory to the sampling site is well defined as being from the south (It is probable that the trajectory with the oval around it is anomalous because we may not be looking at the actual peak concentration which may be to the right of data in the plot). Also, in most cases, the turn in that trajectory to give that approach from the south is not much longer than a few times the distance from the sampling site to the refinery emission point. The hypothesis that this factor identified in the PMF analysis of the February – March data is associated with emissions from the refineries is strongly supported by the back-trajectory data.

It should be pointed out that the great variability of the endpoints of the back trajectories shown in Figure 23, and the short distance of the refineries from the sampling site indicate that a probability analysis of these data would not be useful.

10.3 Correlation with the PMF Unexplained Dichloromethane

In all cases shown in Figure 24 the approach of the trajectory to the sampling site is well defined as being from the south. The hypothesis that the dichloromethane not identified in the PMF analysis is also associated with emissions from the south, southwest with the refineries being the largest point source in this direction is strongly supported by the back-trajectory data. However, as shown in Figure 24, the time periods when peaks in the dichloromethane is present is quite different from the time period when the peaks in the Refinery Associated Dichloromethane factor is present. This analysis only indicates the probable source of the dichloromethane but provides no information on refinery processes associated with the presence of dichloromethane. At least some of the crude oil processed in Utah refineries comes from the Uintah Basin (Utah Department of Environmental Quality, 2019). In 2016, the Uintah Basin produced about 24 million barrels of oil but also produced 78 million barrels of saline (brinyl) non-potable water that required disposal. If there is chlorine coming in with the oil we have all the reactants needed to produce chlorinated methane, including dichloromethane.

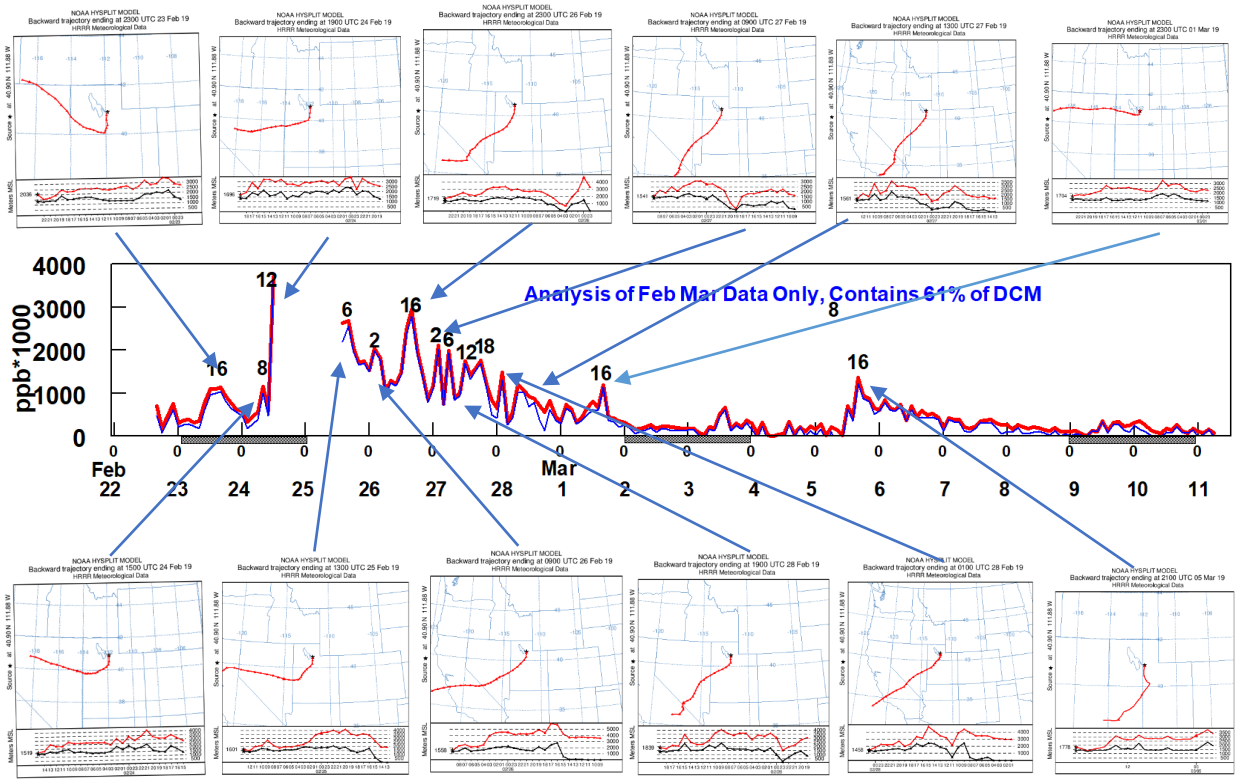

Figure 24. Comparison of the diel pattern for the PMF Unexplained refinery dichloromethane and the back-trajectory corresponing to each identified peak over 200 ppb in the diel pattern.

10.4 Intermittent Emission of Dichloromethane

Evaluation of the diel pattern for dichloromethane emission suggest that the source is intermittent. This finding also agrees with the historical evaluation of DCM levels (Jaramillo et al. 2020). Figure 25 shows the concentration of the Refinery Related Dichloromethane Factor on March 5. Included in this figure are the modeled back wind trajecotries for this same day. At 8 am in the morning a peak reaching 6 ppb of dichloromethane is observed. At this time, the wind trajectory indicates the wind is blowing from the south, southeast. Throughout the day the wind continues to blow from the south, southwest but no peak in the Dichloromethane Factor is observed.

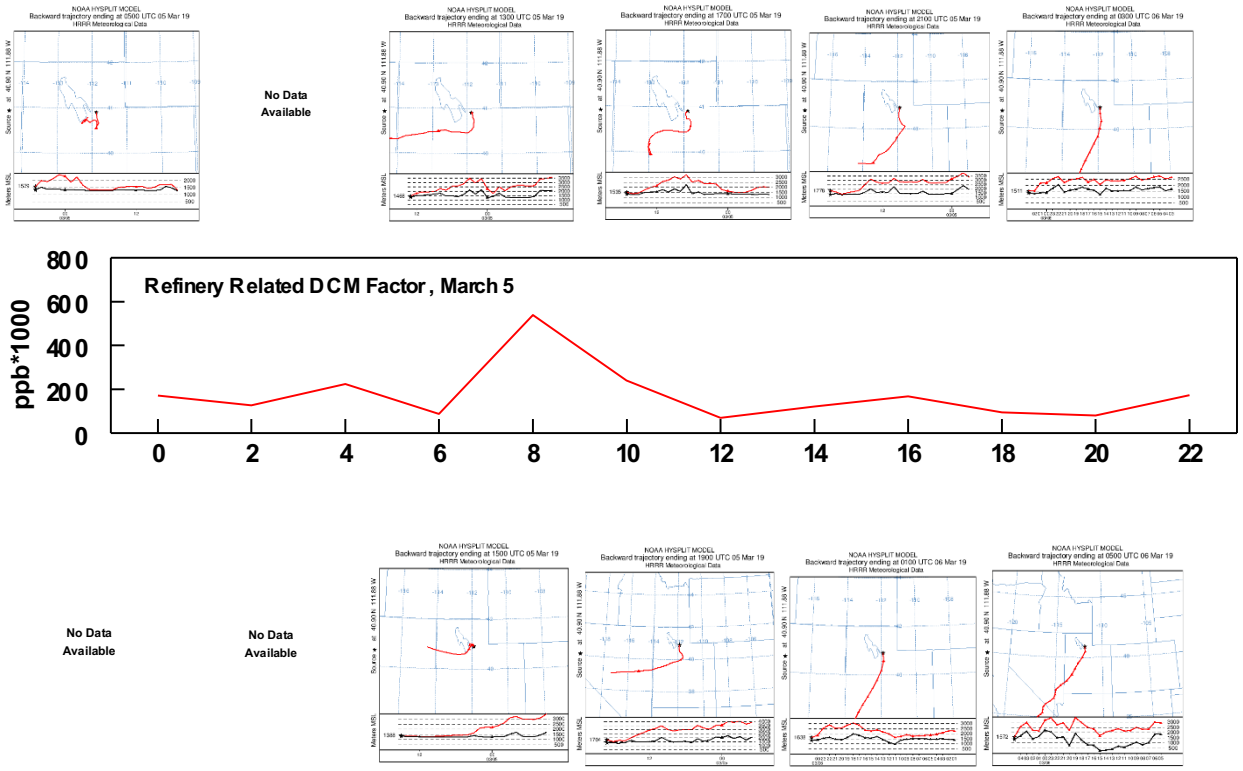

Figure 25. Comparison of the diel pattern for the PMF Unexplained refinery dichloromethane for March 5 and the back-trajectory corresponding to each two hour time period.

This relationship between wind direction and Refinery Related Dichloromethane factor concentrations is not unique to March 5 and is observed at other times. For example, on April 5, 2019 at 12:00 pm a peak in dichloromethane is observed at the same time that the wind is blowing from the south (Figure 26). Modeled back wind trajectories for this day are more stable than on March 5. The wind throughout this day consistently blows from the south but no other peaks in dichloromethane are observed.

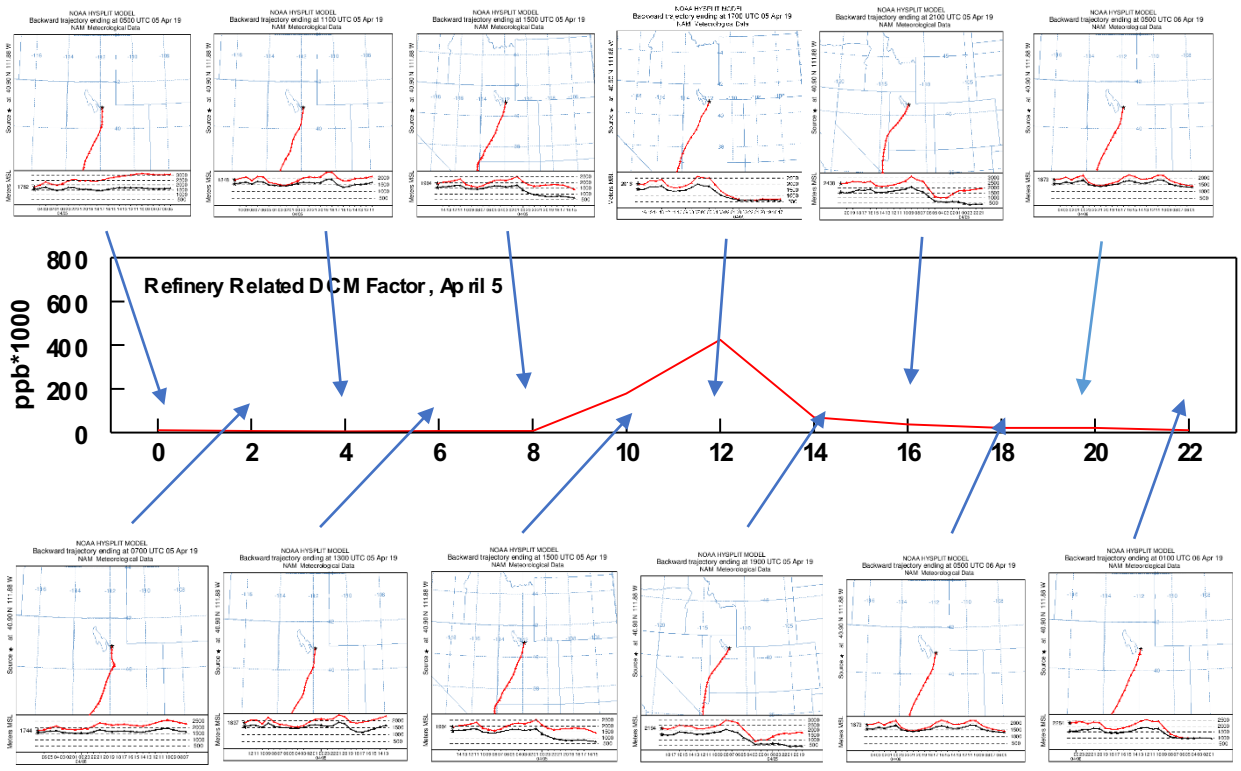

Figure 26. Comparison of the diel pattern for the Refinery Related Dichloromethane Factor April 5 and the back-trajectory corresponing to each two hour time period.

This same pattern is seen for the PMF Unexplained Dichloromethane as is illustrated for the April 26 data in Figure 27.

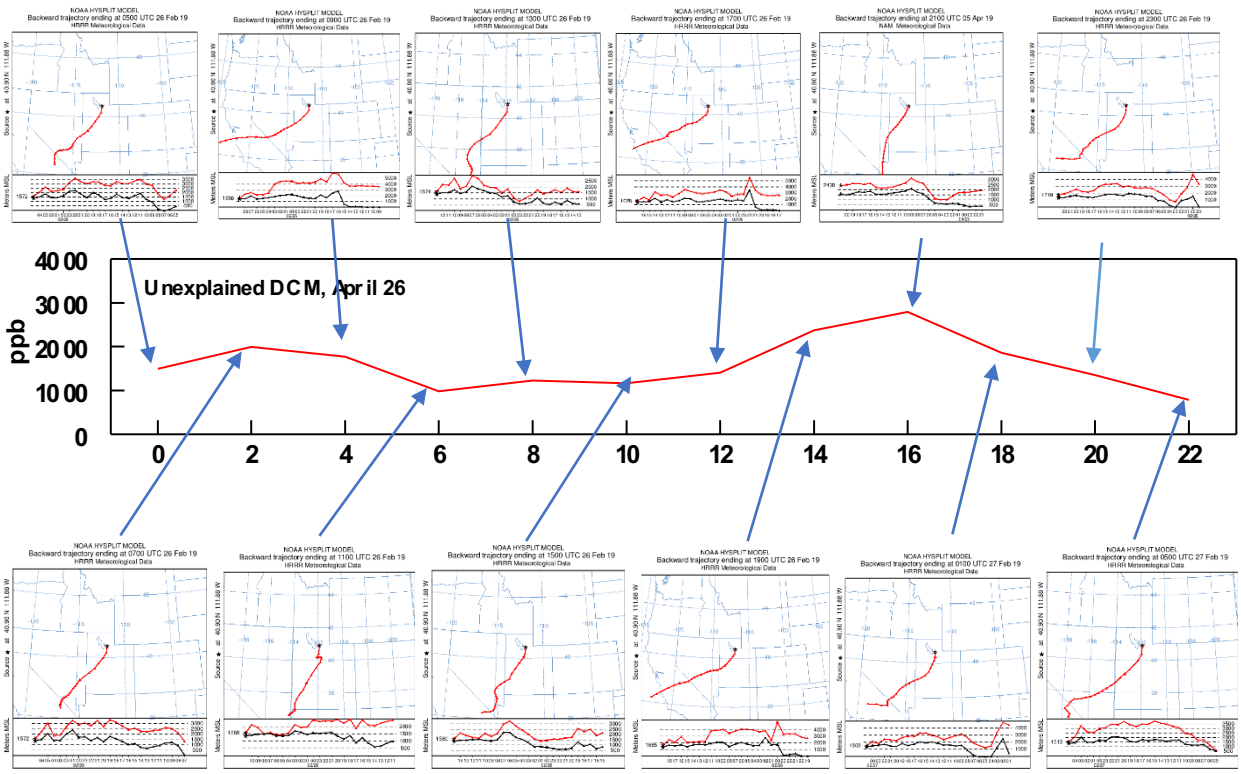

Figure 27. Comparison of the diel pattern for the PMF Unexplained refinery dichloromethane and for April 26 and the back-trajectory corresponing to each two hour time period.

This behavior for both the PMF identified Refinery Related dichloromethane and the PMF Unexplained dichloromethane highlights the intermittent source of dichloromethane that is observed in this study and is consistent with the results of Kelly et al. (Kelly and Daher, 2017, Kelly, 2017) from the 2017 passive sampling study.

10.5 Comparison of Previous DCM Study Results to Current Study

In 2020, Jaramillo et al. performed a source apportionment on 24-hour DCM and air toxics measurements. They also found that DCM comes from an intermittent source but were unable to identify this source. Their study included DCM concentrations that exceeded 2000 ppb, whereas, the DCM levels were in the single ppb range. Because of the large difference in concentrations, it is not possible to determine if the intermittent source suggested in this study is the same as that identified by Jaramillo et al.

In 2017, Kelly (2017) utilized 34 passive samples over a six to seven week period to measure the concentrations of dichloromethane and aldehydes in the Bountiful area. They observed higher concentrations of dichloromethane at sites located in close proximety to the Bounitful Landfill during the first week of the sampling campaign. Analysis of the data collected throughout the entire campaign indicated that the emission source was intermittent. In contrast to the 5-day

averaged sampling time utilized in the first campaign, the current project used results from 1-hour averaged sampling and consequently is expected to provide an improved insight into the sources of dichloromethane.

11. Summary

In the case of the PMF Refinery Associated Factor, the factor is driven by the association of the dichloromethane peaks as observed in Figure 8 and Figure 23 with the species benzene, toluene, ethylbenzene and toluene. This combination is frequently referred to as BTEX, and it should be noted that each of these compounds is not only highly associated with the PMF Refinery Associated Factor, but with each other. BTEX is known to be emitted from petroleum refineries (Baltrenas 2011, Crosby 1998), and the presence of BTEX close to the refineries was suggested from canister samples collected by the saturation study (Kelly and Daher, 2017). However, we are not aware of any publications linking BTEX emission to the emission of dichloromethane. Our results strongly suggest that such a linkage exists and is worthy of verification with additional research.

The difference between probable source identification in this study and the conclusions drawn from the saturation study (Kelly and Daher, 2017, Kelly, 2017) reflect the better correlation which can be made between the appearance of a dichloromethane peaks and the wind direction because of the improvement in sampling time resolution and the availability of back-trajectory analyses.

The consistency of the back trajectories in Figures 20, 23 and 24 is notable. All trajectories clearly approach the sampling site from the south. This leads to the hypothesis that in addition to emissions of dichloromethane associated with BTEX, the unaccounted for dichloromethane may also be associated with emissions from refineries however, recommendations are provided in section 12 that if followed will provide additional clarifying data about other possible contributors located to the south, southwest of the sampling site.

In addition, the consistency of the data in Figures 25-27 indicates that source(s) of both the PMF Refinery Associated Factor and the PMF Unexplained Dichloromethane are intermittent, consistent with results of previous studies (Kelly et al. 2017, Jaramillo et al. 2020). However, it is worth nothing that the very high DCM levels (> 2000 ppb) seen in the Jaramillo study were orders of magnitude larger than those seen in this study. It is possible that the proposed studies outlined in section 12 of this report will provide data that would indicate why we observed lower concentrations of dichloromethane in the present study compared to historic data and if these improvements are due to changes in oil refinery operations or some other factor.

The diurnal pattern observed for formaldehyde suggests that it is coupled to the actinic flux meaning that its formation is driven by the photooxidation of VOC's. The relationship between O_3 and CH_2O supports the conclusion that during this study, formaldehyde was principally formed as a secondary pollutant.

12. Recommendations

The above hypotheses can be further tested and better understood by additional research involving:

- Collection of 24-hour (or shorter) samples of dichloromethane at the Bountiful sampling site and a corresponding site south of the refineries to see of a pattern of impact at one or the other, but not both sites can be identified.
- Evaluation of current State data on emissions of BTEX from the refineries to see if we can identify the processes which may dominate in determining the emissions of BTEX.
- If the state does not have complete current data on emissions of BTEX from the refineries which will allow the identification given in the previous bullet, such emission inventory data should be obtained.
- Fence-line or other appropriate sampling to see if emission of dichloromethane from the refineries can be established and if we can identify which part of the refinery is associated with the emissions and if emissions are similar from each of the refineries.
- Evaluation of the new data and the inventory data for BTEX to see if we can identify why the concentrations of the dichloromethane not accounted for in the PMF analysis was so different during the April as compared to the February – March periods of the 2019 Bountiful study.

References

Baltrenas, Pranas; Baltrenaite, Edita; Serevicience, Vaida; Pereira, Paulo; (2011) "Atmospheric BTEX concentrations in the vicinity of the crude oil refinery of the Baltic region" *Environ Monit Assess* **182**,115-127

Centers for Disease Control and Prevention. (2012, May 2). *Carcinogen List*. Retrieved February 10, 2017, from The National Institute for Occupational Safety and Health (NIOSH): https://www.cdc.gov/niosh/topics/cancer/npotocca.html

Cropper P.M., Eatough D.J., Overson D.K., Hansen J.C., Caka F., Cary R.A. (2018) "Use of a Gas Chromatography-Mass Spectrometry Organic Aerosol Monitor for In-Field Detection of Fine Particulate Organic Compounds in Source Apportionment" *J. Air Waste Manage. Assoc*. **68**, 390-402.

Cropper P.M., Bhardwaj N., Overson, D.K., Hansen J.C. and Eatough D.J. (2019) "Source Apportionment analysis of Winter 2016 Neil Armstrong Academy Data (West Valley city, Utah), *Atmos. Environ.*, in press.

Crosby, D.G. Environmental toxicology and chemistry, New York: Oxford University Press (1998)

EPA 2014 "EPA Positive Matrix Factorization (PMF) 5.0 Fundamentals and User Guide", Gary Morris, Rachelle Duvall, Steve Brown and Song Bia, EPA/600/r-14. September 2014, www.epa.gov

Grover B.D. and Eatough D.J. (2008) "Source Apportionment of One-Hour Semi-Continuous Data Using Positive Matrix Factorization with Total Mass (Nonvolatile plus Semi-Volatile) Measured by the R&P FDMS Monitor" *Aerosol Sci & Technol.*, **42,** 28-39

Grover B., Eatough N.L., Hopke P.K., Eatough D.J. (2008). "Measurement of Fine Particulate Mass, Including the Semi-Volatile Constituents, with a GRIMM Monitor," Proceedings, Measurements Symposium, Air and Waste Management Association, Paper # 51

Jaramillo, I.C., Kerry, K, Hansen, J., Bhardwaj, N., Eatough, D., Thalman, R., and Daher, N, Identifying Sources of Dichloromethane and Formaldehyde in the Bountiful Region, Poster Presented at the Science for Solutions Conference, March 2019

Jaramillo, I.C., Kelly, K., Daher, N., Hansen, J., Eatough, D.J. (2020) "Bountiful City Dichloromethane Source Apportionment Study" Air Quality: Science for Solutions 4 abstract

Kelly, K and Daher N. (2017) Saturation Air Toxics Monitoring in Davis County, Utah, Final Report submitted to Utah Department of Air Quality

Kelly, K., Watts, M., Wangsa, R., Phan, T. (2017) Improved Understanding of Potentially Carcinogenic Air Pollution in Bountiful Through Data analysis.

Kotchenruther, R.A. (2016) "Source apportionment of PM2.5 at multiple Northwest U.S. sites:

Assessing regional winter wood smoke impacts from residential wood combustion" *Atmospheric Environment*, **142**, 210-219

Kuprov, R. (2016, July 6). *2015 Special Toxics Study Report.* Retrieved February 10, 2017, from Utah Department of Air Quality: http://www.deq.utah.gov/Pollutants/H/haps/docs/2015-Special-Toxics-Study.pdf

Polissar A. V., Hopke P. K., Malm W. C., Sisler J. F. (1998) "Atmospheric Aerosol over Alaska 2. Elemental Composition and Sources" *J. Geophys. Research* **103**, 19045-10057

Utah Department of Environmental Quality website (2019). https://deq.utah.gov/general/petroleum

Utah Geological Survey, Chidsey, T.C Jr. (2018) "Oil and Gas in the Uinta Basin, Utah-What to do with the Produced Water" https://geology.utah.gov/map-pub/survey-notes/uinta-basin-produced-water/